Chapter 4
Climate and Drought in Turkey

Murat Turkes

Abstract The aim of this section of the book is to make a scientific synthesis of the climate of Turkey along with the aridity and drought conditions, in a contemporary physical geographical, hydro-climatological and meteorological approach. The Mediterranean macroclimate, including much of Turkish territory, mainly results from the seasonal alternation between mid-latitude frontal cyclones associated with polar air masses during the winter, the subtropical high pressure systems link to subsiding maritime tropical air mass over the mid-north Atlantic, and the continental tropical air masses over the Northern Africa during the summer. In addition to these pressure and circulation conditions, the north-western surface and/or circulation-based extensions of the Asiatic monsoonal low pressure system cause generally very dry and hot conditions over the Eastern Mediterranean and the Middle East regions, including the southern and central parts of Turkey. According to the Köppen-Geiger climate classification, the southern and western portions (Marmara, Aegean, Mediterranean and South-eastern Anatolia regions) of Turkey are characterized mainly with the dry summer sub-tropical Mediterranean climate (Csa). All of these regions are also influenced by mid-to-high degree drought probability and drought risk, while the Black Sea Region is characterized with a mid-latitude temperate climate with a low-level drought probability and risk. The probabilities of being extremely-dry evidently indicate maximum values on the coast of Mediterranean Sea and over the border zone between Turkey and Syria with a highest probability of about 0.27. Continental steppe and cold snowy climates are dominated over most of the Central and Eastern Anatolia regions.

Keywords Mediterranean and Turkey climates · North Atlantic oscillation · Composite precipitation anomalies and 500 hpa anomalous circulations · Drylands · Drought probability · Vulnerability/risk of Turkey

---

M. Turkes (✉)
Center for Climate Change and Policy Studies, Bogazici University, Istanbul, Turkey
e-mail: murat.turkes@boun.edu.tr

N. B. Harmancioglu, D. Altinbilek (eds.), *Water Resources of Turkey*, World Water Resources 2, https://doi.org/10.1007/978-3-030-11729-0_4

4.1 Introduction

The present Mediterranean-type macroclimates of the Earth mainly result from the seasonal alternation between mid-latitude frontal cyclones associated with polar air masses during the winter, and subtropical high pressure systems related with subsiding maritime and continental tropical air masses during the summer. When considering the 'true' Mediterranean macro-climate, in addition to these pressure and circulation conditions, the north-western surface and/or circulation-based extensions of the Asiatic monsoonal low pressure system (Fig. 4.6) cause generally very dry and hot conditions over the Eastern Mediterranean and the Middle East regions, including the southern and central parts of Turkey, during the 5-month warm period of the year from May to September (Turkes 1998, 1999, 2003, 2010).

Nature, magnitude and variability of precipitation amounts and air temperatures are generally associated with the location, variation and activity of the atmospheric centers of action throughout the year (except summer) over most of the Mediterranean regions and Turkey (Iyigun et al. 2013; Kutiel et al. 2001; Kutiel and Turkes 2005; Turkes 1996, 1998, 2003; Turkes et al. 2002a; Turkes and Erlat 2003, 2005, 2008, 2009; Turkes and Tatli 2009; Turkes et al. 2009; Xoplaki 2002; Xoplaki et al. 2004; Erlat and Turkes 2012, 2013; etc.). In addition to the humid-temperate Black Sea climate and the continental inland climates, there are various Mediterranean and Mediterranean-like climate types in Turkey. Two major factors cause this evident climate diversity in Turkey. First, Turkey is situated in a transition zone that is under the influence of various atmospheric disturbances and weather types originating from polar and tropical regions. The second factor is the complexity of topographical features, rapid elevation changes within short distances, the land-sea interactions, and finally thermodynamic influences and modifications caused directly by the Mediterranean Sea at the south and the Black Sea at the north. The zonal soils in Turkey are distributed over the country in accordance with the spatial distribution patterns of the major climate types along with the lithology (parent material), geomorphology and vegetation formations.

The aim of this chaper is to provide a comprehensive picture of the climate types and aridity, and spatial and temporal variability in dryness and drought conditions of Turkey and its relatively nearby surrounding regions with different physical geographical conditions. These regions are characterized mainly with the mid-latitude and the Mediterranean macro climates primarily according to the Köppen-Geiger climate classification, the United Nations Environmental Program and the United Nations Convention to Combat Desertification Aridity Index (UNEP/UNCCD *AI*), and the Standardized Precipitation Index (*SPI*). Climatological and meteorological assessments have consisted of the dominant permanent and/or semi-permanent atmospheric pressure and circulation conditions. This chapter also includes some basic points of general soil characteristics of Turkey with respect to climate.

4.2 Data and Methodology

4.2.1 Data

For the station-based climate data of Turkey, long-term average monthly precipitation totals and monthly mean temperature data were calculated by using the long-term monthly precipitation totals and monthly mean temperature series, which were originally developed by Turkes (1996, 1999, 2013) and Turkes et al. (2002b), respectively. Detailed information on meta-data and homogeneity analyses applied to long-term precipitation and temperature series of Turkey can be found in Turkes (1996, 1999, 2013) and Turkes et al. (2002b, 2009), respectively.

4.2.2 Methodology

4.2.2.1 The Köppen-Geiger Climate Classification System

The Köppen-Geiger Climate Classification System (Köppen 1936; Köppen and Geiger 1954) is the most widely used tool of climatic classifications for physical geographical and environmental (climatological, biogeographical, ecological, etc.) purposes. We accepted in this section the criteria that follow Köppen's last publication about his classification system in the Köppen-Geiger Handbook (Köppen 1936), with the exception of the boundary between the temperate (***C***) and cold (***D***) climates, because we used the Köppen-Geiger climate data computed by Peel et al. (2007). Peel et al. (2007) followed Russell (1931) and used the temperature of the coldest month > 0 °C, rather than > −3 °C as used by Köppen in defining the temperate – cold climate boundary (see Wilcock 1968; Essenwanger 2001 for a history of this modification).

The Köppen-Geiger climate system consists of a shorthand code of letters designating major climate groups, subgroups within the major groups, and also subdivisions to differentiate particular seasonal characteristics of air temperature and precipitation. In the system, five major climate groups are determined by capital letters as follows, where the groups ***A***, ***C*** and ***D*** have sufficient heat (energy) and precipitation amounts for growth of forests and wood-land vegetation formations:

- ***A* Humid Tropical Climates**: Mean air temperature of the coldest month is above 18 °C ($T_{cold} \geq 18$ °C). Tropical ***A*** climates have no winter season. Annual rainfall amount is large enough to exceed annual potential evapotranspiration (*PET*) amount.
- ***B* Arid (Dry) Climates**: *PET* exceeds precipitation on the average conditions throughout the year. No water surplus occurs in the annual water balance; consequently, no permanent streams develop in the Arid ***B*** climate regions, with some regional exceptions such as in the Central Anatolia region of Turkey characterized mainly by a ***BS*** climate.

- ***C*** **Mid-latitude Warm Temperate (Mesothermal) Climates:** The coldest month has a mean air temperature below 18 °C, but above 0 °C (0 °C < T_{cold} < 18 °C); at least 1 month has a mean temperature above 10 °C (T_{hot} > 10 °C). Temperate ***C*** climates hence have both an evident summer and an evident winter season.
- ***D*** **Cold (Snow) (Microthermal) Climates**: The coldest month mean air temperature is under 0 °C ($T_{cold} \leq$ 0 °C), and the mean air temperature of the warmest month is above 10 °C (T_{hot} > 10 °C). The 10 °C isotherm also coincides approximately with pole-ward limit of forest growth.
- ***E*** **Polar (Ice) Climates**: Mean air temperature of the coldest month is under 0 °C (T_{cold} < 0 °C), and the mean temperature of the warmest month is below 10 °C (T_{hot} < 10 °C). The polar ***E*** climates have no true summer.

In the Köppen-Geiger climate system, subgroups of the five major groups are indicated by a second letter according to the following codes:

- ***S*** **Steppe Climates**: Semi-arid climates with long-term mean annual precipitation amount varying from 350 mm to 700 mm at the low latitudes. Exact precipitation boundary is determined by a formula considering temperature.
- ***W*** **Desert Climates**: An arid climate mostly having mean annual rainfall amount less than 250 mm. The exact boundary of steppe climate is also determined by a formula.
- The letters ***S*** and ***W*** are applied only to the arid (dry) ***B*** climates yielding two important combinations as ***BS*** and ***BW***.
- ***f*** **Moist Climate Without Dry Season**: Adequate precipitation amount in all months. This modifier letter is applied to ***A***, ***C*** and ***D*** groups of major climates.
- ***m*** **Monsoon Climate with a Short Dry Season**: Tropical rainforest climate in spite of short and dry winter in the monsoonal precipitation regime cycle, particularly in the monsoon Asia. It applies only to ***A*** climates.
- ***w*** **Dry Winter Climate**: Dry season happens in winter of the respective hemisphere (low-sun season).
- ***s*** **Dry Summer Climate**: Dry season is in summer of the respective hemisphere (high-sun season), mostly associated with the subtropical high pressure systems (e.g. Azores high for the Mediterranean Basin and its surrounding regions). It applies to ***C*** and ***D*** major climates.

From combinations of the two letter groups, 13 distinct climates of the Köppen-Geiger classification appear as in the Table 4.1. Finally, Köppen added a third letter to the code group of his classification (not given here).

4.2.2.2 The UNEP/UNCCD Aridity Index

Arid, semi-arid and dry sub-humid climates were defined as "areas, other than polar and sub-polar regions, in which the ratio of annual precipitation to potential evapotranspiration falls within the range from 0.05 to 0.65" for the purposes of the United

Table 4.1 Two-letter Group Climates of the Köppen-Geiger Classification with a Short Description[a]

- ***Af***: **Tropical rainforest climate**
- ***Am***: **Tropical monsoon climate** (a variant of ***Af*** with a short dry season)
- ***Aw***: **Tropical savanna climate**
- ***BW***: **Desert climate**
- ***BS***: **Steppe climate**
- ***Cs***: **Temperate rainy climate with dry summer** (humid mesothermal) or **Mediterranean climate** (dry summer subtropical)
- ***Cw***: **Temperate rainy climate with dry winter** (humid mesothermal)
- ***Cf***: **Temperate rainy climate without dry season** (humid mesothermal) or **humid temperature west coast**
- ***Ds***: **Cold snowy forest climate with dry summer** (humid microthermal).
- ***Dw***: **Cold snowy forest climate with dry winter** (humid microthermal)
- ***Df:*** **Cold snowy forest climate humid in all seasons** (humid microthermal)
- ***ET*** **Polar tundra climate**
- ***EF*** **Polar forest climate**

[a]*The groups with in the Köppen-Geiger climate system, framed with red boxes, show climate types that are found in Turkey*

Nations Convention to Combat Desertification (UNCCD 1995). In the present study, *UNEP/UNCCD Aridity Index (AI)* is used as one of the base methods for determining dry-land types in Turkey and assessing their vulnerability to the desertification processes.

Following UNEP (1993), *AI* is written as:

$$AI = \left(\frac{P}{PET}\right) \tag{4.1}$$

where P and PET are annual precipitation and potential evapotranspiration totals (mm), respectively. The *PET* values were estimated by taking the approach used in the WATBUG program into consideration, which was developed by Willmott (1977) for climatic water budget, and Thornthwaite's climate classification (1948). The *AI* values below 1.0 show an annual moisture deficit in average climate conditions. The criteria in Table 4.2 were used to characterize the dry-lands of Turkey (Turkes 1999).

4.2.2.3 Drought Probability Based on Standardized Precipitation Index

In the classical approach for obtaining the Standardized Precipitation Index (*SPI*), the cumulative distribution function (*CDF*) of precipitation totals are formed from the fitted frequency distribution according to McKee et al. (1993, 1995), and then the probabilities from the fitted *CDF* are transformed to standard normal distribution by using inverse standard normal distribution. Consequently, this is a method consisting of a transformation of one probability distribution to another. In this common methodology, the gamma distribution is widely used (e.g. Thom 1966; McKee et al. 1993, 1995; Wilks 1995; Guttman 1998, 1999; Turkes and Tatli 2009, etc.).

Table 4.2 Dry land (arid climate) types in Turkey according to the Aridity Index (AI) and their vulnerability to desertification. (Turkes 1999)

Aridity criteria	Dry land type	Assessment
$0.20 \leq AI < 0.50$	Semi-arid areas	Vulnerable to desertification
$0.50 \leq AI < 0.65$	Dry sub-humid areas	Vulnerable to desertification
$0.65 \leq AI < 0.80$	Sub-humid areas	Vulnerable to desertification

On the other hand, Turkes and Tatli (2009) proposed a new *SPI* approach for obtaining the local-time means from maxima and minima envelopes of the monthly total precipitation series for calculation of the *SPI* series. This proposed new *SPI* technic is an analogical methodology of the empirical mode decomposition (*EMD*). It was initially proposed for the study of ocean waves by Huang et al. (1998) and Wu et al. (2007). This approach was made use of by many researchers in the atmosphere and climate sciences (e.g., Zhu et al. 1997, 2001; Coughlin and Tung 2001, 2004; Turkes and Tatli 2009). The basic (climatological) drought probability used in this study is based on the monthly series of the proposed new *SPI*, which had been calculated before by Turkes and Tatli (2008, 2009) for the 96 stations of Turkey.

4.3 Results and Synthesis

4.3.1 Physical Geographical Settings

Turkey is located between 36–42° northern latitude and 26–45° eastern longitude in the Northern Hemisphere (Fig. 4.1). Accordingly, there is a 76-minute local time difference between the west and the east of the country. According to the Turkish Statistics Institute, Turkey's total surface area is 785,347 km^2 and the total area of Turkey without natural lakes and is 769,604 km^2 (TurkStat 2016). Turkey is composed of seven geographical regions. According to the ranks of their surface area, these are of the Eastern Anatolia Region, Central Anatolia Region, Black Sea Region, Mediterranean Region, Aegean Region, Marmara Region and the Southeastern Anatolia Region (Fig. 4.1). Because it is located in the southern part of the mid-latitude geographical belt towards the sub-tropical belt, four seasons are experienced distinctively during the year. The territory of Turkey is located between Europe and Asia. Turkey's land borders are 2949 km long in total. The coastal border of the peninsula, which is surrounded by three sides with the Black Sea at the north, the Aegean Sea at the west and the Mediterranean at the south, is 8592 km except the islands.

Turkey is a country of highlands with an average altitude of 1141 m at an average slope of 17%, varying generally from 3% to 30% (Elibuyuk and Erkan 2010). This figure of the average altitude of the country is higher than the average altitude of each continent on the Earth. Turkey's most flat region is the South-eastern Anatolia; the lowest region is the Marmara; the greatest sloppy (the most gradient) region is the Black Sea; the highest one is the East Anatolia Region (Fig. 4.1).

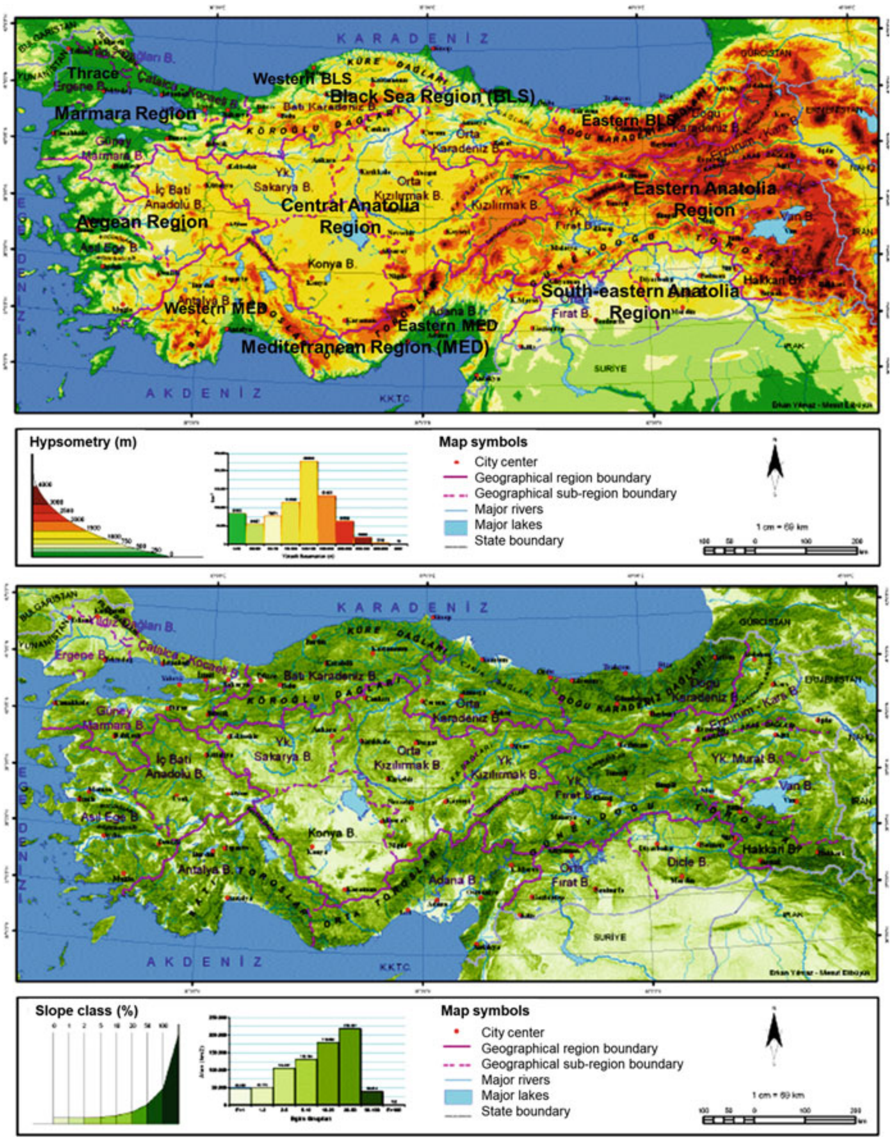

Fig. 4.1 (**a**) Altitude steps (hypsometry in meter) and (**b**) Slope classes (in percent, %) the boundary lines of the geographical regions and sub-regions (shortly B on the maps) of Turkey. (Elibuyuk and Erkan 2010)

The geological evolution of Turkey, which is situated on the Alpine-Himalayan mountain ranges or orogenetic belt geologically, had begun towards the late Palaeozoic period and continues its completion today, during the post Quaternary period. Mountains cover a great portion of the country's land. It is clearly seen that the high mountain chains, which are namely the North Anatolian Mountains at the north, and the Mediterranean Taurus Mountains and the South-eastern Tauruses at the south, stretch along the northern and southern coastal zones from east to west making wide arches. Those mountain ranges at the Mediterranean and Black Sea regions are generally perpendicular to the coastal zones. The middle part of the country consists of the Anatolian Plateau (Fig. 4.1). This plateau separates the high mountain ranges at the north and south from each other, although they traverse them in the east. For this reason, the eastern part of the country is higher and more mountainous than the remaining parts. On the other hand, there are many plains and low basins in the inner parts of the country, and coastal plains and delta-flood plains along the coastal zone. Deltas formed by the Kizilirmak and Yesilirmak rivers and the Adana plain can be given as examples of the large coastal plains in the country. According to the orogenetic belt classification studies made for Turkey, Turkey as a whole is located in the Mediterranean section of the Alpine orogenetic belt (Ilhan 1976; Ketin 1983, 1994). This orogenetic belt was situated between the Eurasian plate at the north and the African and Arabian platforms at the south. Plate tectonics theory provides a better understanding of the geologic and morphotectonic evolutions of Turkey and its nearby surrounding. The plate tectonics is realized by the approaching and collision of two plates in the subduction zones, causing sediment deposits and magmatic rocks having a thickness of thousands of meters (Ketin 1994). The complex Alpine–Himalayan orogenetic belt, on which Turkey also is located, had formed as a result of the faster movement and approaching of large pieces of Gondwanaland plate in the south (i.e., African, Arabian, Indian, etc.) than that of the Eurasian plate (including the platforms of Russia, Siberia, etc.) and by folding, faulting and uplifting of the Alpine–Himalayan geosyncline's deposits by the orogenic process (Erinc 1982). The Arabian–Eurasian convergence is an important process for better understanding of the geologic/geomorphologic evolution and neo-tectonic fundamentals of Turkey. Final collision of the Arabian–Eurasian (here, Anatolian sub-plate) had taken place in the Miocene epoch (Sengor 1980).

Ketin (1966), in his study to determine the tectonic units of the Anatolian Peninsula, divided Turkey into four tectonic units, which are namely the Pontid (the northern Anatolia and Marmara regions), the Anatolid (the Central Anatolia region), the Torid (Tauruses and other Mediterranean mountains), and the Border Folds (the South-eastern Tauruses and South-eastern Anatolia region). Ketin (1966) found out that tectonics and orogenic development in the Anatolian Peninsula had slowly progressed from north to south. The first severe orogenic movements had started in the northern Anatolia and Marmara regions and, in the following period, had spread towards the Central Anatolia, Tauruses and at last towards the South-eastern Tauruses, which is the youngest orogenic mountain belt of Turkey geologically. The South-eastern Tauruses tectonic unit had completed its main formation in the late Miocene epoch, and even the Pliocene layers joined into the folding movement. It is evident that the old Central Anatolia land region had played a role of inner massif after the Eocene epoch and made a significant contribution to the orography of the Taurus Mountains (Ketin 1966, 1983; Erinc 1982).

4.3.2 General Meteorology and Climate Dynamics

In this sub-section, general meteorological and climate dynamic aspects and the occurrence and classification of the macro Mediterranean and Turkish climates are explained. Mediterranean climates are mostly considered under the climates of **Group *C*** Mid-latitude warm temperate (mesothermal) climates according to the Köppen's climate classification (Table 4.1). The mid-latitude climates are controlled mainly by both tropical and polar air masses and weather systems according to the Strahler's (1973) genetic climate classification (Group II). This classification was mainly developed, based on the global and regional atmospheric circulation conditions, air-masses, and mid-latitude cyclones and anticyclones, etc. (Figs. 4.2 and 4.3) (Turkes 2010). The mid-latitude temperate (mild) climates are located in parts of the latitude range between 30° and 60° in either hemisphere, where the term mild (temperate) refers to the winter temperatures and not necessarily to those of the summer.

These warm temperate climates are those of the middle latitudes, dominating the planetary polar front zone during at least half of the year, particularly from the late autumn to middle-spring, over which both tropical and polar air masses and weather patterns extend and dominate. The geographical zone in which the mid-latitude climates prevail is mainly subject to frontal low-pressure systems (mid-latitude cyclones). Most of the precipitation, in particular in winter, in these climate regions occurs associated with the frontal precipitation events through the mid-latitude cyclones. Average annual total precipitation amounts of the warm temperate climates are modest, ranging from about 350 mm on the equator-ward margin and in some inland areas (in far eastern inland areas) to about 650 mm at the pole-ward margin. However, it is over 1000 mm over the high-mountainous regions of the northern Mediterranean basin, for example on the Mediterranean Sea coast of Turkey and southern wind-ward side of the Alps, due to the topographically induced precipitation in addition to the frontal precipitation events (Turkes 2010).

4.3.2.1 Occurrence and Spatial Patterns of the Mid-Latitude Temperate Climates

The mid-latitude temperate climates have the greatest temporal variability, varying from a few days to several weeks. Seasonal variability (i.e. seasonality) is also evident in these climates, whereas the seasonality lacks both in the tropics with the almost constant heat gain and the almost-continuous cold of the polar (i.e. Arctic and Antarctic) regions. The mid-latitude regions are mainly characterized with frequently alternating incursions of tropical (T) and polar (P) air masses throughout the year (Fig. 4.1). This apparent regional circulation dynamic produces more convergence movements than anywhere else with the exception of the equator. Seasonal alternation of the tropical and polar air-masses controls changes and variability in frequency and intensity of the Rossby waves and associated weather

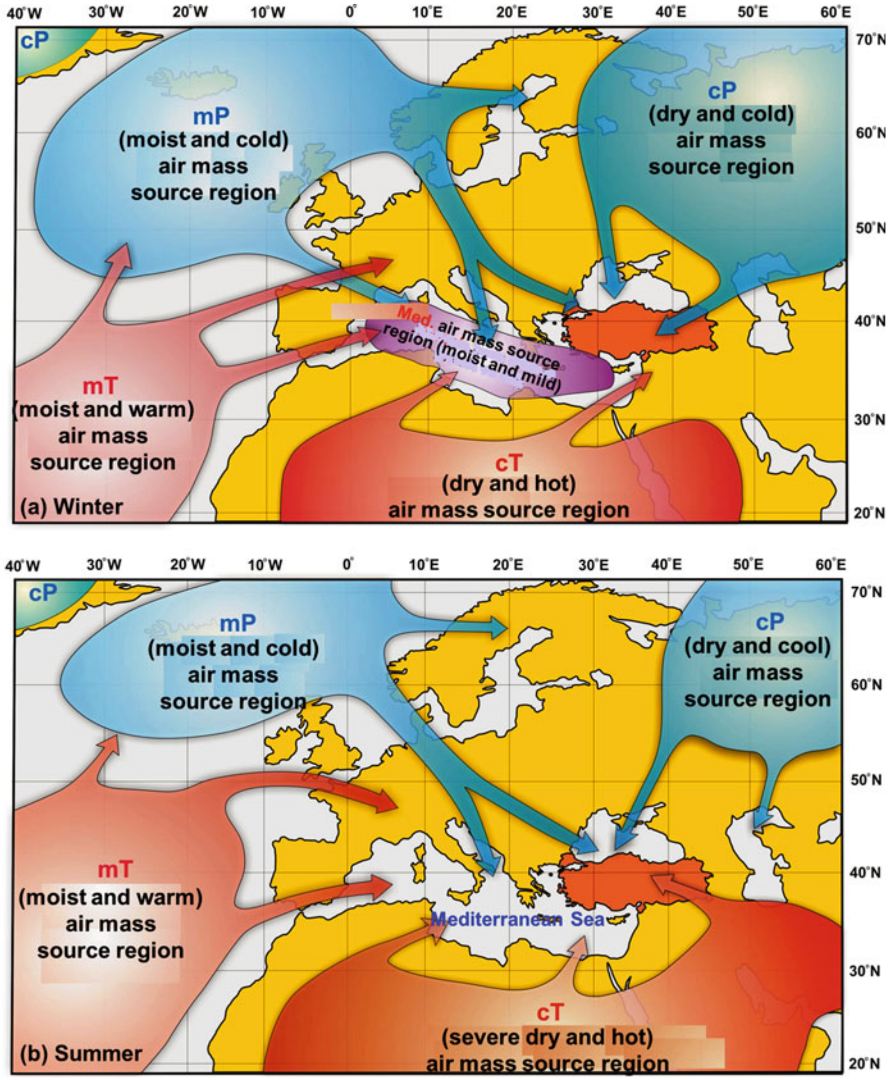

Fig. 4.2 Seasonal changes in climatology of air masses over the Mediterranean Basin and surrounding regions due to changes in planetary and synoptic scale surface and tropospheric pressure and wind systems driven by the apparent movements of Sun and associated migration of the Intertropical Convergence Zone (ITCZ) between (**a**) Winter and (**b**) Summer. (rearranged in English from Turkes 2010)

systems of mostly dynamic originated cyclonic and anticyclonic nature (Erinc 1969; Barry and Chorley 2003; Turkes 1998, 2010; Sahin et al. 2015; Lolis and Turkes 2016). The seasonal rhythm of the surface air temperature regime in the Mediterranean climate is usually more prominent than that of the precipitation regime.

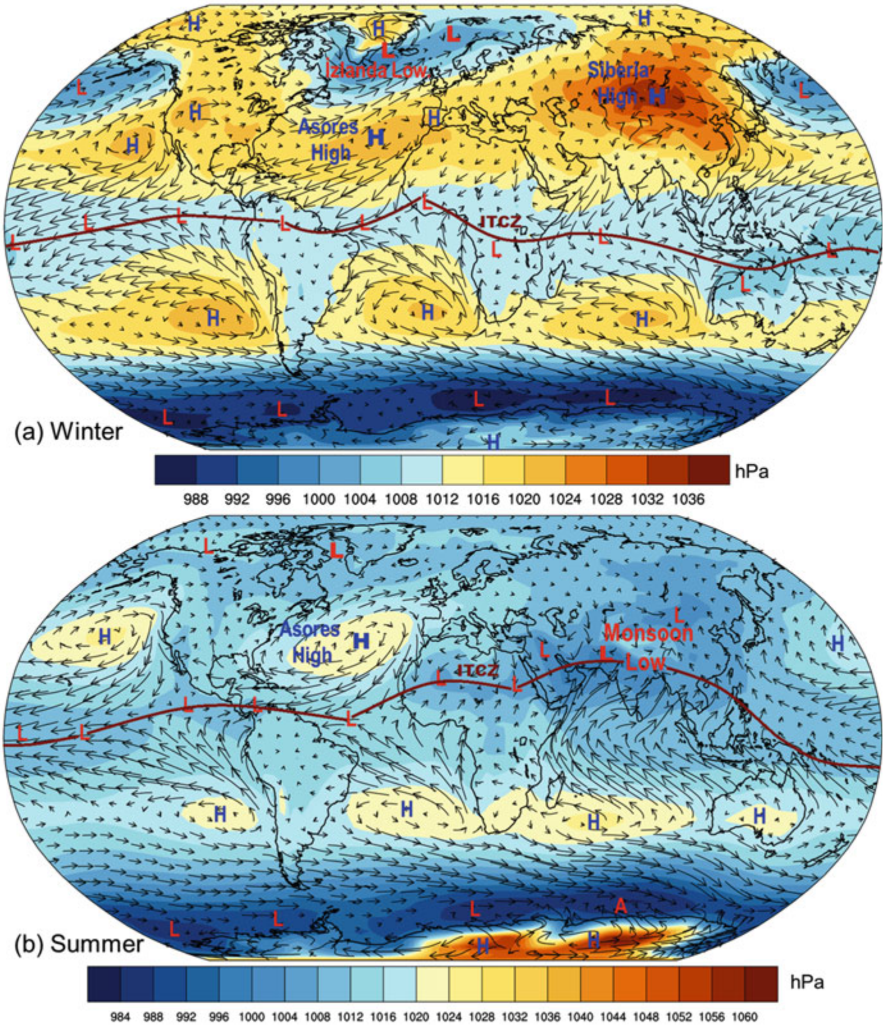

Fig. 4.3 Seasonal changes in climatology of the global surface air pressure and wind circulation systems associated with the apparent migration of the Intertropical Convergence Zone (ITCZ) between (**a**) Winter and (**b**) Summer. (rearranged in English from Turkes 2017a)

The mid-latitude climates occupy the equator-ward margin of the mid-latitudes, occasionally extending into the subtropics and being elongated pole-ward in some western coastal areas due to the high topographic barriers. They clearly constitute a transition between warmer tropical climates of the south and colder mid-latitude climates of the farther north. Summers in these climates are long and warm or hot, while winters are usually short and relatively mild. High variability in both precipitation total amounts and seasonal distribution over the ***C climates*** is characteristics.

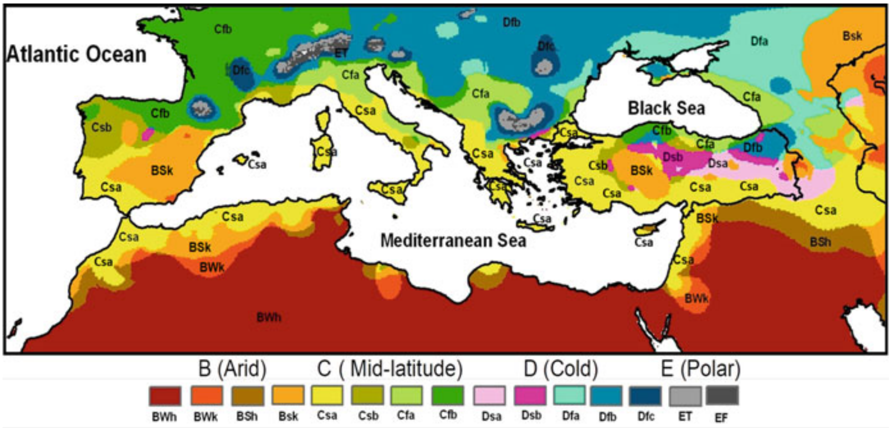

Fig. 4.4 Geographical distribution of climate types over the Mediterranean Basin and surrounding regions according to the three-letter symbols of the Köppen-Geiger classification. [From Turkes (2017a) re-drawn by making use of the data by Peel et al. (2007)]

The temperate warm ***C climates*** are subdivided into three types primarily on the basis of precipitation amounts (limits) and seasonality, and secondarily on the basis of some air temperature limits and temperature seasonality: Mediterranean (***Csa***, ***Csb***), humid subtropical (Cfa, Cwa), and marine west coast (Cfb, Cfc), all of which are found in the Mediterranean Basin (Fig. 4.4).

The Mediterranean basin is significantly important for understanding the climate, climate variability, hydrological cycle, and future climate change and variability over a large region, associated with many nearby countries including Turkey, because of its links with the large-scale atmospheric and oceanic teleconnections and circulations (Sahin et al. 2015). The genesis of the Mediterranean macroclimate (shortly the Mediterranean climate) is mainly associated with the seasonal migrations of the mostly dynamic-originated pressure systems (i.e. centers of action) (Fig. 4.3) and the alternating tropical and polar air masses between summer and winter (Fig. 4.2). Consequently, the dry summer subtropical Mediterranean climates can be mostly found along the west coasts between about 25° and 40° latitudes as a natural part of the mid-latitude temperate climates (Turkes 2017a).

The largest Mediterranean climate region of the Earth is found in the Mediterranean Basin, which can thus be called as the ‘true’ Mediterranean macroclimate mainly due to the topographic features of the subtropical westward of the continents (Turkes 2017a). In the Atlantic-ward of the southern Europe and the Mediterranean Sea Basin, there are no north to south oriented mountain chains, and the Mediterranean climates penetrate a great distance from the west basin of the Mediterranean Sea, with some parts of the Iberia Peninsula, to the East Basin of the Mediterranean Sea and the Mediterranean coastal and inland regions of the Middle East region (Fig. 4.4). Although the term Mediterranean is used to describe the climate synonymous with the region surrounding the Mediterranean Sea, it is not exclusive to this region. The Mediterranean climates are also found, for example, in the northern Iran,

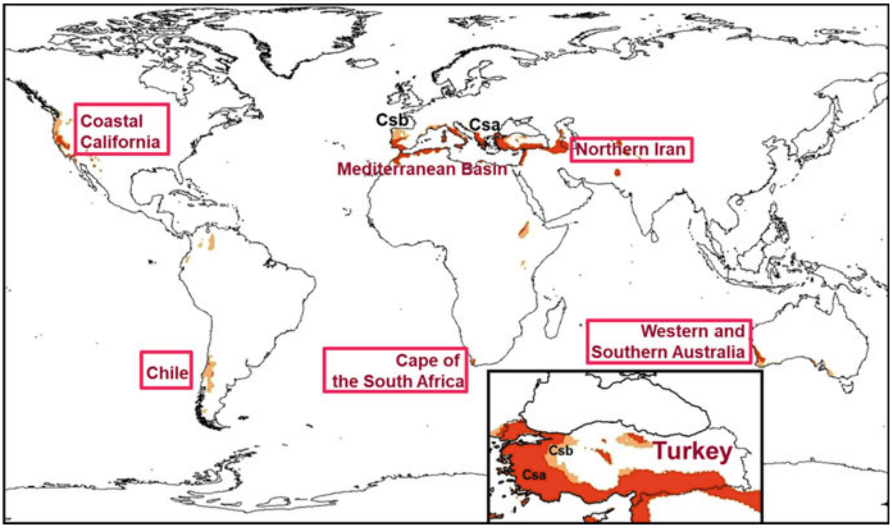

Fig. 4.5 Geographical distribution of the Mediterranean and the Mediterranean-like climate regions over the world. (Turkes 2010)

California, Chile, Australia, New Zealand and South Africa, in addition to the 'true' Mediterranean regions of Portugal, Spain, Coastal North-west Africa (Morocco, Tunisia, Algeria), France, Italy, Greece, Turkey, Lebanon and Israel (Fig. 4.5) (Turkes 2010; Turkes et al. 2011). These regions are mostly dominated in summer by dry, stable and subsiding air from the eastern portions of dynamic originated subtropical highs, which is also the sinking branch of the Hadley cell circulation. In winter, the wind and pressure systems shift equator-ward as a result of the equator-ward migration of the Rossby waves and associated polar jet streams and upper air westerlies with the polar front. The Mediterranean climate regions are influenced by the westerlies with their trailing mid-latitude frontal cyclones (Turkes 2010).

Seasonality is the most dominant and distinctive character and factor of the Mediterranean climates (Turuncoglu et al. 2018). The Mediterranean climate tends to alternate wet and dry seasons, because it is located over the transitional zone between the dry west coast tropical desert, mainly related with the subtropical high pressure systems, and the descending segment of the tropical Hadley circulation cell, and the wet west coast climate mainly related with the polar front and associated mid-latitude cyclones.

As we shortly discussed the mid-latitude climates above, there are many atmospheric features that can be considered for dominating the Mediterranean climates. For instance, the Rossby waves, which are formed by the upper air troughs and lows, and the upper air ridges and highs, controlled penetration of polar air masses [continental polar (cP), maritime polar (mP), and very rarely continental Arctic (cA)] towards equator at certain months of the year, and tropical air masses [continental tropical (cT), and maritime tropical (mT)] towards poles at other certain months of the year (Fig. 4.2). In this respect, the seasonal movements arising from mainly the Sun's seasonal migration (i.e., Sun's apparent movement) and thus the amount and intensity of the Sun's radiation resulting in an energy exchange between the poles and the equatorial belt are the main mechanisms (Turkes 2010). On the other hand, due to the seasonal movements of the inter-tropical convergence zone (ITCZ) associated closely with the movements of the Sun (Fig. 4.3), the Rossby waves would be closer to the equatorial belt in winter than that in summer. Thus, polar originated weather systems can more strongly fluctuate to further equator-ward in winter than in summer. This fluctuation is also responsible in enhancing the seasonal energy contrasts globally, particularly over the continents.

In the mid-latitudes, while the planetary-scale Rossby waves, the upper air jet streams governing also westerlies and the frontal cyclones are the most powerful features of these climates, these atmospheric controls are also themselves controlled by topography, continentality, land-sea distribution and interactions, air masses, and their thermo-dynamics and mechanical modifications arising from the physical geographical features of the Earth surfaces (Turkes 2010). Consequently, there is no simple explanation of the mid-latitude climates including the Mediterranean climate as a whole.

Almost all precipitation comes from the frontal cyclones, except for the late spring and early summer convective instability showers and thunderstorms in inland Mediterranean climates of the Anatolia Peninsula and the Middle-East region. On the other hand, the Alp Mountains of the South Europe and the North Anatolia and Taurus mountains of Turkey create stronger influence on the westerly and northerly air-flows and associated mid-latitude frontal cyclones by means of the orographic lifting of the moist air masses. This mechanism leads adiabatic cooling and condensation of water vapor of air masses, and occurrence of the precipitation over the mountains, particularly by the time of that faced to southerly and westerly moist air masses (Turkes 1996, 1998, 2010).

4.3.2.2 Dry-Summer Subtropical Mediterranean Climates

The Mediterranean climate, ***Cs*** of the main Köppen classification ***Group C*** and the climate number 8 of the Strahler's classification ***Group I*** (Strahler 1973; Turkes 2010) are mainly characterized with warm to hot dry summers and cool to cold wet winters.

Most Mediterranean climates of the Earth are classified as ***Csa***, which means that summers are hot with mid-summer monthly averages between 24 °C and 29 °C and high maximums above 38 °C. Average cold-month temperatures are about 10 °C with occasional minimums below freezing temperatures.

The coastal Mediterranean climate regions have much milder summers than the inland Mediterranean climate regions. This is mostly due to sea breezes in some coastal areas as a result of being adjacent to cool currents associated with the permanent anticyclonic circulation of the subtropical high pressure systems located over the subtropical oceans of the Earth. These coastal Mediterranean climates are classified as ***Csb***. In the coastal areas, the hot-month mean air temperatures lie between 16 °C and 21 °C. ***Csb*** winters are slightly milder than ***Csa*** winters, the former having cold-month mean air temperatures of about 13 °C. ***Csb*** regions also have higher humidity, frequent advection and evaporation fogs, and occasional low *stratus*, *altostratus* and *nimbostratus* overcast.

Marine west coast ***Cf climates*** located at the pole-ward of the Mediterranean climate region (Fig. 4.4) occur as a result of persistent influences by the mid-latitude frontal cyclones during the year. Consequently, marine-west coast climate regions are mostly characterized with windy, cloudy and rainy conditions almost around the year. On the average conditions, these climates are cooler than their equator-ward neighbor climates.

Based on all the explanations above, we may summarize the Mediterranean climates with following five distinctive characteristics (Turkes 2010; Turuncoglu et al. 2018):

(1) About half of the modest annual precipitation amount falls in winter, whereas summers are mostly virtually rainless.
(2) Winter temperatures are unusually mild for the mid-latitudes except some eastern and inland regions; summer air temperatures vary from hot to warm.
(3) Cloudless skies and intensive sunshine (shortwave solar radiation) are typical particularly in summer months.
(4) It has major influences from sea and land distribution and the interactions between sea and lands, in addition to the ocean-atmosphere interaction, during the year particularly in the 'true' or 'actual' Mediterranean macro climate region, etc.
(5) The major characteristics of the Mediterranean climate is the high temporal variability at seasonal and inter-annual to centennial scales due to following factors (Turkes 2010):

- It extends in a transition region between temperate and cold mid-latitudes and tropics (i.e. subtropical zone);
- It faces significant circulation (associated pressure and wind systems characterizing mid-latitude and tropical/monsoonal (Fig. 4.6) weather and climate, respectively) changes between winter and summer;
- It is closely associated with several atmospheric oscillation and/or teleconnection patterns during the year, where they vary depending on seasons, such as North Atlantic Oscillation (NAO), Arctic Oscillation (AO), Mediterranean Oscillation (MO), El Niño-Southern Oscillation (ENSO), and North Sea – Caspian Pattern (NCP), etc. (e.g., Kutiel and Turkes 2005; Turkes 1998; Turkes and Erlat 2003, 2005, 2006, 2008, 2009, 2018a, b; Trigo et al. 2006; Erlat and Turkes 2012, 2016; Sahin et al. 2015, etc.).

Regarding the last bullet above, recent studies indicated that the NAO is one of the major atmospheric sources for the spatial and temporal variability of the

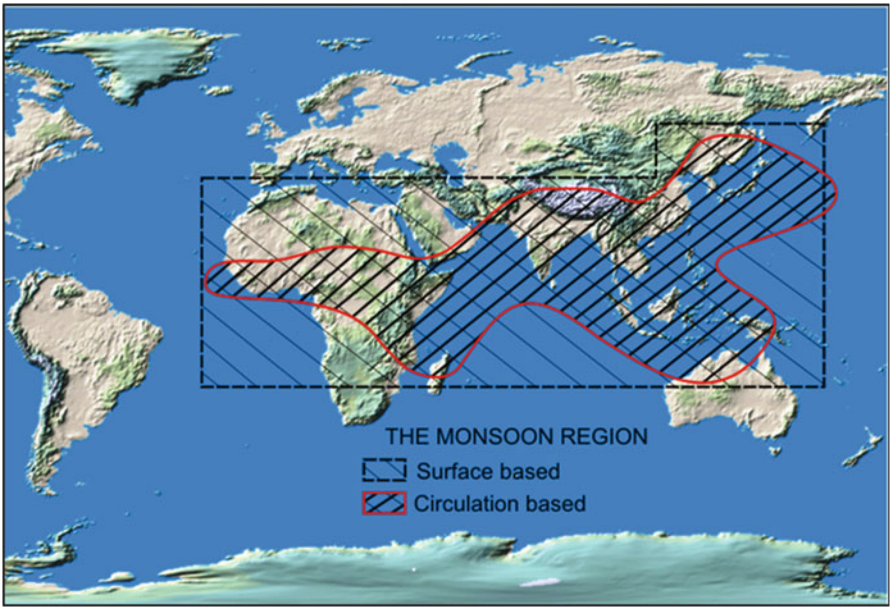

Fig. 4.6 Schematic illustration for the geographical extends of the direct circulation-based and indirect surface-based influences of the major monsoon systems (Monsoonal Lows) during the year, and the area of their observed influences on the Mediterranean Basin and Turkey. [Henderson-Sellers and Robinson (1986): re-arranged and plotted on a new base map by making some modifications]

precipitation conditions in Turkey, including significant wet periods and meteorological droughts (Turkes and Erlat 2003, 2005, 2006; Sahin et al. 2015; Turkes 2014a, b, etc.).

The NAO, which is associated with the surface pressure see-saw or oscillation among two large-scale dynamic centers of action, so called the Azores High and the Icelandic Low, is a well-known atmospheric teleconnection pattern (Turkes and Erlat 2003). The NAOIs are developed in order to evaluate behavior of the NAO and regional climate anomalies linked to the extreme NAO episodes. A NAO index (NAOI) is generally arranged based on the difference of normalized sea level pressure (SLP) anomalies between a station in the area of the Azores and another one in Iceland. Another NAOI is also calculated by using the difference of the normalized SLP between a station located in the Iberian Peninsula and another in Iceland (Turkes and Erlat 2005). The Ponta Delgada-Reykjavk (PD-R) NAOI was used in this study, because Turkes and Erlat (2005, 2006) found that the PD-R NAOI is the best NAOI among the three NAOI compared [i.e. PD-R, L-S(R) and Gibraltar-Reykjavk (G-R)], with respect to the ability of controlling variability in precipitation series of Turkey, particularly for winter precipitation.

When the NAO is in its extreme phases, both the Icelandic Low and the Azores High are well developed during cool/cold period of the year, especially in winter

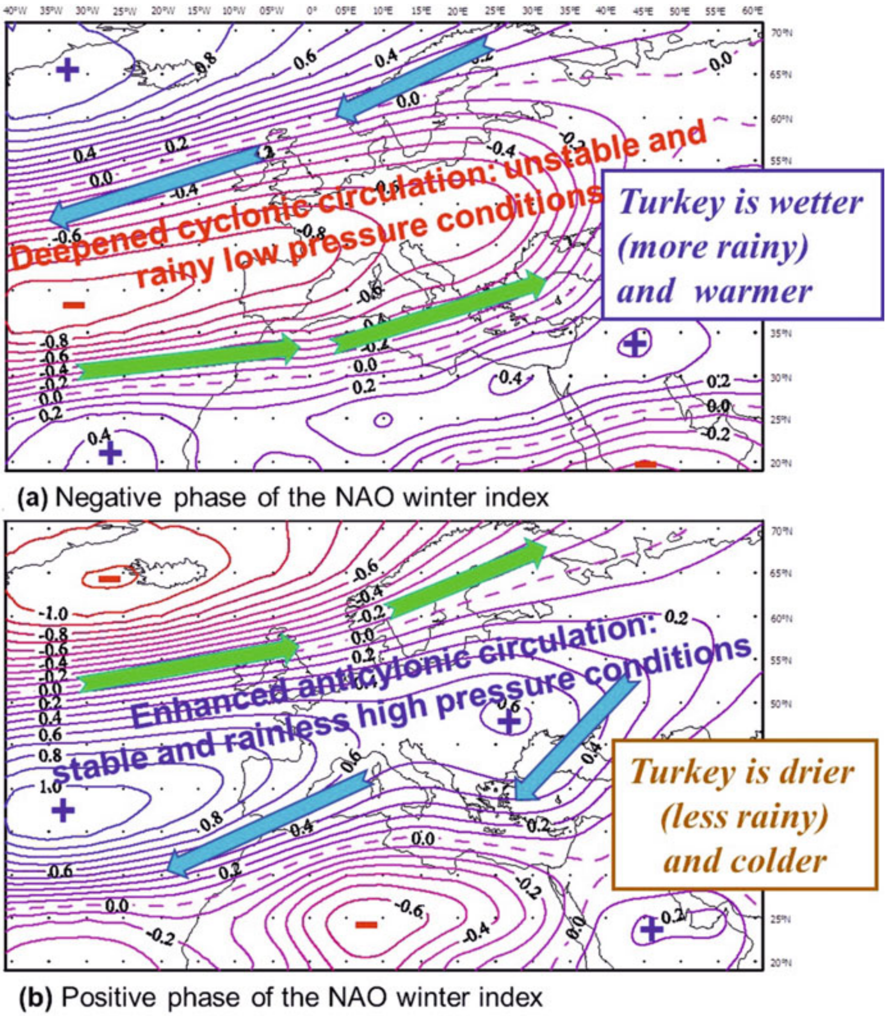

Fig. 4.7 Geographical distributions of composite winter 500-hPa geopotential height anomalies during (**a**) the negative phase and (**b**) the positive phase of the Ponta Delgada–Reykjavik (PD-R) NAO winter index. [re-drawn and re-arranged from Turkes and Erlat (2009)]

(Fig. 4.7). The negative phase of the NAO indicates stronger-than-average westerly and south-westerly circulation over the subtropical north-east Atlantic, North Africa and the Mediterranean basin towards Turkey, and the stronger-than-average north-easterly circulation across Scandinavia and the mid-latitude and sub-Arctic north-east Atlantic, particularly in winter, spring and annually (Fig. 4.7a). On the contrary, the positive phase of the NAO shows the increased westerlies over the mid-latitudes and Scandinavia and increased easterly and north-easterly circulation over a large conveyer zone from Turkey to the subtropical Atlantic via the Mediterranean basin and North Africa (Figs. 4.7b and 4.8).

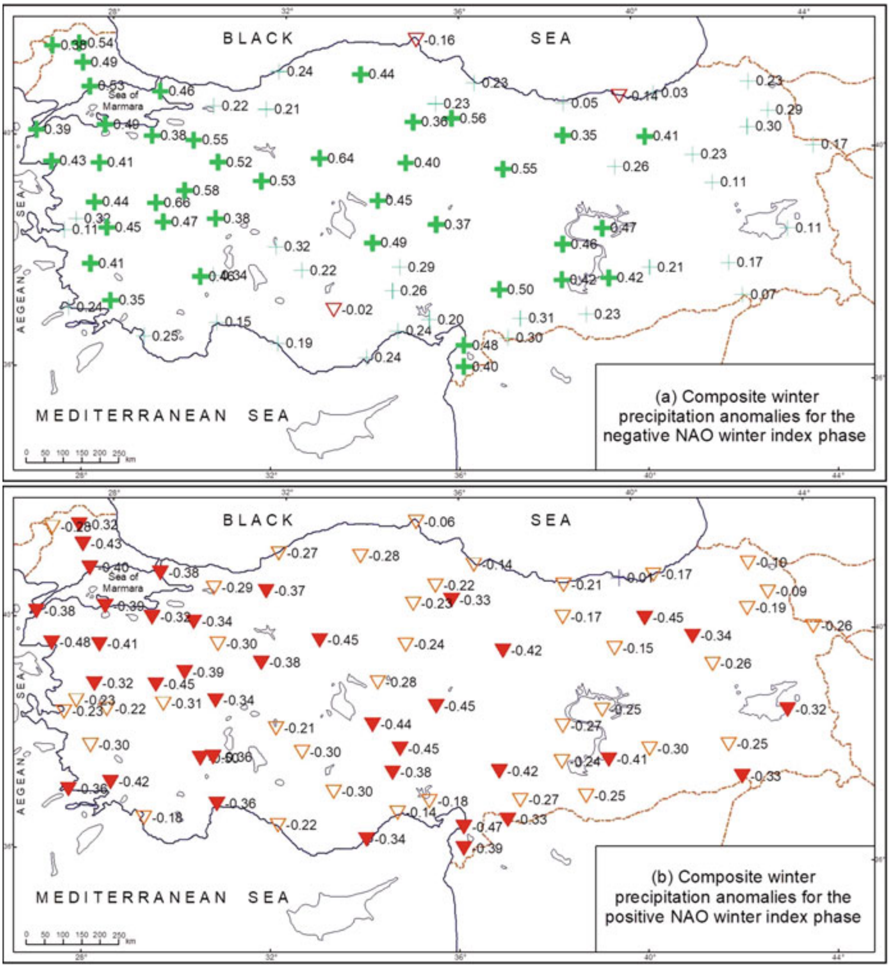

Fig. 4.8 Geographical distribution patterns of composite precipitation anomalies, (**a**) during the weak and (**b**) the strong phases of the NAO winter index. (Turkes and Erlat 2003)
Bold plus symbols (filled inverse triangles) show significant wetter (drier) than long-term average precipitation conditions at the 0.05 level of significance, according to Cramer's test

Individual widespread and significant wet conditions and meteorological drought events in the cold months of the year in Turkey, particularly in winter, are mostly controlled by the extreme NAO conditions (Figs. 4.7, 4.9 and 4.10). According to the studies performed by Turkes and Erlat (2003, 2005, 2006) and Turkes (2014a, b, 2016), the 500-hPa circulation corresponding to the negative NAOI phase brings above long-term average precipitation to Turkey in winter (Fig. 4.8a), spring, autumn, and annually. This circulation is associated with the NAO pattern in which the 500-hPa geopotential level is anomalously high in the area of the Icelandic Low and anomalously low across the regions of the Azores High and Europe in

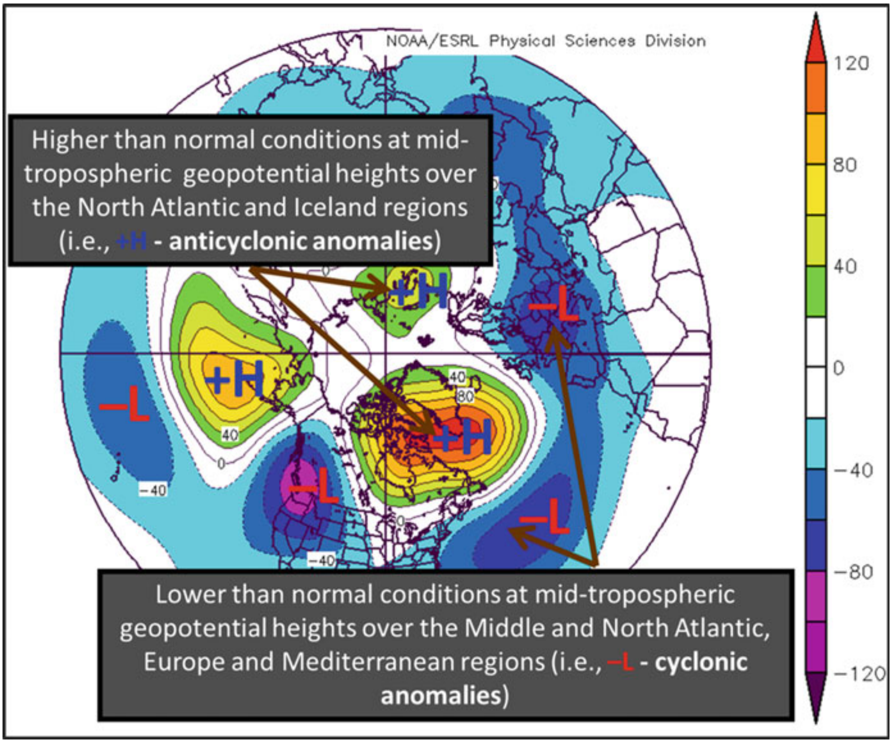

Fig. 4.9 Anomalies pattern of 500 hPa geopotential height level during the 1969 winter season (December 1968 to February 1969) with respect to the 1981–2010 climatology over the Regions of the Europe, Mediterranean and Turkey, which pointed out an example of the anomalies mid-tropospheric circulation anomalies associated with the weak (negative) phase of the year-to-year variability in the NAO. In Turkey, this pattern leaded occurrence of the geographically coherent large-scale and significant *positive precipitation anomaly* in 1969 (**strong wet year**). [See: Fig. 4.11(a)]

general (Fig. 4.7a). On the contrary, the anomalous circulation pattern corresponding to the positive NAOI phase over the North Atlantic and Europe is responsible for the drier than long-term average precipitation conditions in Turkey, particularly in winter (Fig. 4.8b), when the 500-hPa geopotential level is anomalously low over the area of the Icelandic Low and anomalously high across the subtropical and mid-latitude north-east Atlantic and the European regions (Fig. 4.7b). In other words, when the NAO is in its extreme low-index (negative) value, winters in Turkey tend to be generally wet (rainy) (Fig. 4.8a), whereas winters in Turkey tend to be experienced generally with drought (rainless) conditions when the temporal pattern of the NAO is in its extreme high-index (positive) value (Fig. 4.8b).

Considering the extreme NAO events for the period 1940–2015, it is very likely that widespread strong wet conditions in some or most regions of Turkey during the winters of 1940–1942, 1956, 1963, 1966, 1969, 1970, and 2010–2011 were detected

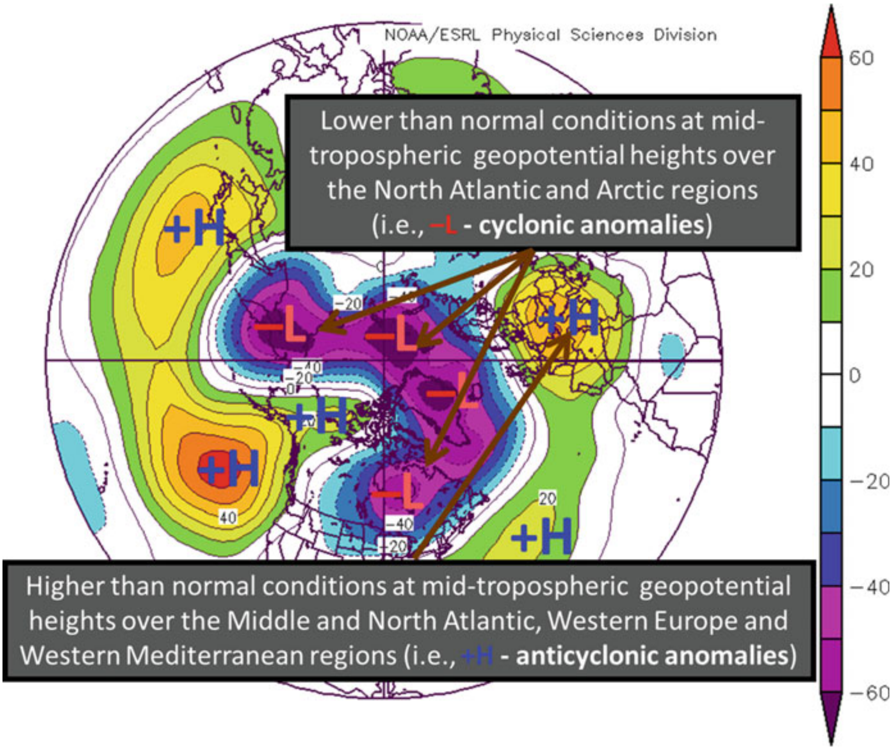

Fig. 4.10 Anomalies pattern of 500 hPa geopotential height level during the 1989 winter season (December 1988 to February 1989) with respect to the 1981–2010 climatology over the Regions of the Europe, Mediterranean and Turkey, which pointed out an example of the anomalies mid-tropospheric circulation anomalies associated with the strong (positive) phase of the year-to-year variability in the NAO. In Turkey, this pattern leaded occurrence of the geographically coherent large-scale and significant *negative precipitation anomaly* in 1989 (**strong drought or dry year**). [See: Fig. 4.11b]

to match the extreme low-index values in the same winter seasons of at least two NAOIs. On the other hand, it is possible to explain that geographically coherent severe droughts in some or most regions of Turkey during the winters of 1943, 1957, 1973, 1974, 1983, 1989, 1990, 1992, 1993, 1994, 2007–2008, and 2013 were closely related with the extreme high-index values of the NAO indices. In this respect, according to Turkes and Erlat (2005) for instance, during the weakest winter index of the three NAOIs in 1969 (Fig. 4.9), positive precipitation anomalies (wet conditions) exhibited a coherent distribution pattern over much of Turkey, indicating a mixed distribution of very much above and extremely above long-term average precipitation conditions (Fig. 4.11a). On the other hand, it is very likely that geographically the largest severe drought events occurred in the winter of 1973 (not shown here) and in the successive winters of 1989 and 1990. The most severe and coherent widespread drought event (Fig. 4.11b) appeared during the strongest NAO event in 1989 (Fig. 4.10).

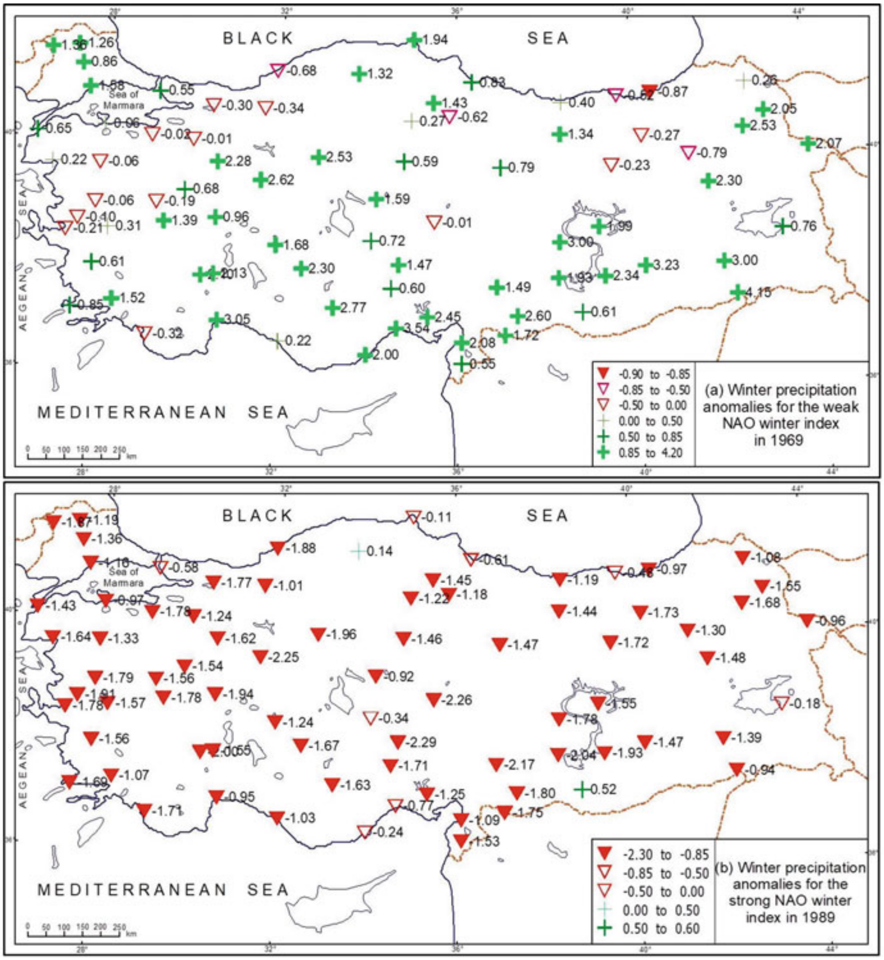

Fig. 4.11 Geographical distribution patterns of normalized winter precipitation anomalies in Turkey, during the weak and strong NAO winter indices in the years of (**a**) 1969 and (**b**) 1989. (Turkes and Erlat 2005). *Bold plus symbols (filled inverse triangles) show considerable wetter (drier) than long-term average precipitation conditions*

4.3.2.3 Turkish Climate

As we already discussed above, the major climate of the Mediterranean Basin including Turkey arises mainly from an unequivocal seasonal alteration from winter to summer between mid-latitudes and sub-tropical/tropical pressure and wind systems (circulation patterns). Thus, there is a highly seasonal precipitation regime in the western and southern regions of Turkey, characterized mainly by dry and hot summers (Turkes 2010). During the summer, the weather and climate in most regions of Turkey, particularly in the Mediterranean and the continental steppe

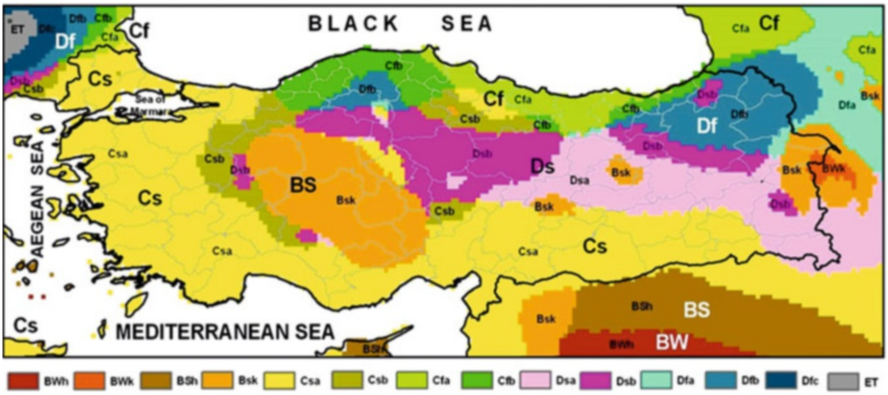

Fig. 4.12 Geographical distributions of climate types in Turkey based on the first, second and third hand letters classification of the Köppen-Geiger climate system. (Turkes 2010)

climate types over the western, central and southern Turkey, are influenced by the pole-ward descending branch of the tropical Hadley cell producing clear, stable, warm and dry cloudless conditions associated with the subsiding and adiabatically warm air masses. Cold fronts or troughs of the trailing mid-latitude cyclones and the convective instability thunder-storms, which are associated with the dynamically originated deep and cold-nuclei upper-air lows and troughs and related with relatively cold air masses, cause occurrence of the summer convectional rainfall over the continental Central and Eastern Anatolia regions along with the inland Mediterranean climate regions. Types of precipitation events (i.e. hydrometeors) are mostly strong rainfall, rain-showers, hail-storms and thunder-storms with heavy rain and hail events.

In winter, however, trailing mid-latitude cyclones are responsible for most of the precipitation events and amounts over the regions. Topographic influences over the mountain chains facing the prevailing weather systems, such as Alps and Atlas Mountains in general, and the North Anatolian Mountains, the Mediterranean Taurus Mountains, and the South-east Tauruses in the north and south of Turkey, significantly contribute to increase the amount, frequency and intensity of the precipitation over these regions with the temperate rainy west coast (Black Sea in Turkey) and the Mediterranean climates, respectively. Cold spells are usually linked to both mP and cP air masses. Winter mP air masses are considerably less cold than cP air, and it may give cool, cloudy and wet conditions, while the cP air may produce cold, stable and dry conditions (Turkes 2010).

The climate of Turkey according to the Köppen-Geiger climate system is considerably diverse (Fig. 4.12), as in many other climate classifications of Turkey. When only the first and the second-hand letters in classification of the Köppen-Geiger climate system are considered, the following major climate types can be identified (Turkes 2010):

(1) **Sub-tropical steppe climate *BS*** (mostly ***BSk***) in Turkey is found in the mid-part of the continental Central Anatolia region and the Van-Igdir district over most-eastern part of the continental Eastern Anatolia region (Fig. 4.12).
(2) **Temperate rainy or humid temperature west coast climate without dry season *Cf*** (mostly ***Cfa*** and ***Cfb***) (humid mesothermal) dominates the Black Sea coastal region of Turkey with the exception of the western sub-region (Fig. 4.12).
(3) The Marmara, Aegean, Mediterranean and the South-eastern Anatolia regions and the western and southern portions (i.e. some parts of the Sakarya and Konya sub-regions) of the continental Central Anatolia Region belong to the **dry summer subtropical Mediterranean climate or temperate rainy climate with dry summers** (humid mesothermal) ***Cs*** (mostly ***Csa***) (Fig. 4.12). Yearly soil-moisture deficiency is not characteristic in **Group *C* climates** in general, whereas seasonal soil-moisture deficiency, particularly in summer months, is evident in the Mediterranean ***Csa*** and ***Csb*** climates due to changes in the hemispheric and regional circulation, air mass and pressure systems producing dry conditions in the summer months.
(4) On the other hand, a **cold snowy forest climate with dry summers** (humid microthermal) ***Ds*** (mostly ***Dsa*** and ***Dsb***) takes place over a relatively large zone on the mid-northern portions of the continental Central and Eastern Anatolia regions of Turkey; whereas a **cold snowy forest climate humid in all seasons** (humid microthermal) ***Df*** (mostly ***Dfb***) exists over relatively small areas seen in the northern portions of the continental Central Anatolia region and the north-eastern Anatolia sub-region (mostly Erzurum-Kars sub-region) of Turkey (Fig. 4.12).

In theory, and according to the UNEP/UNCCD Aridity Index (*AI*), *AI* values below 1.0 generally show an annual moisture (soil water) deficit in average climatic conditions, whereas *AI* values above 1.0 generally show an annual moisture surplus (Fig. 4.13).

The maritime influences on the weather and climate conditions of Turkey are characterized mainly with the mP and mT air masses (Fig. 4.2). In winter, Mediterranean air masses carried by the westerly air flows (W, SW and NWerly) tend to decrease towards the continental inland regions, including the Central, Eastern and South-eastern Anatolia regions of Turkey. Major changes of the inland Mediterranean regions reflect a decrease of precipitation amounts in winter and the number of rainy days, and an increase of precipitation amounts in spring months, particularly with continentality, such as that in the mid-west and south parts of the Central Anatolia Region and the South-eastern Anatolia Region of Turkey. The Northern Anatolia Mountains, on the other hand, separate the Mediterranean, steppe and cold snowy forest climates from the west coast temperate rainy (Black Sea in Turkey) climate, while the Tauruses and the South-eastern Taurus Mountains separate the Mediterranean climate (***Csa***) from the more continental Mediterranean climate (***Csb***), steppe and cold snowy forest climates to the north and the east of the Anatolian Peninsula (Fig. 4.12).

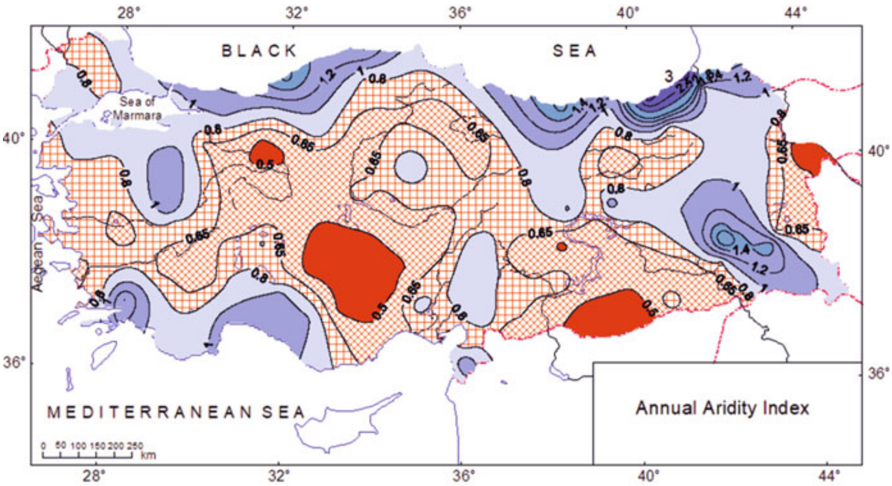

Fig. 4.13 Geographical distribution of the UNEP/UNCCD aridity indices of the 151 climatological and meteorological stations in Turkey, in which arid, semi-arid, dry sub-humid and sub-humid areas of the country are highlighted by hatching with the red color. [Re-arranged in English from Turkes (2013)]

In Turkey, dry sub-humid climatic conditions extend throughout most of the Continental Central Anatolia and South-eastern Anatolia regions, some part of the eastern Mediterranean, and eastern and western parts of the Continental Eastern Anatolia region; while the semi-arid climatic conditions are found only in the Konya Plain and the Igdir district of the Eastern Anatolia region (Fig. 4.13). The areas having values $0.65 < AI < 0.80$, where an annual soil moisture deficit exists, are also concentrated around the semi-arid and dry sub-humid areas of Turkey. The arid-lands in Turkey having *AI* values between 0.20 and 0.80 are likely to have been influenced by the desertification processes (Table 4.2), by considering the existing hydroclimatological conditions, human-induced land degradation, observed and projected climate change and variability, etc. (e.g., Ozturk et al. 2012, 2015; Topcu et al. 2010; Sen et al. 2012; Turkes 1999, 2010, 2013, 2017b, c; Dengiz 2018; Turkes and Akgunduz 2011).

4.3.3 Climatological Drought Probabilities in Turkey

In this sub-section, the long-term climatological *SPI* probabilities in Turkey, calculated by using the monthly *SPI* series, are discussed through considering the SPI classes of below-normal, normal, above-normal, generally dry and wet, extremely-wet and extremely-dry, as given in Table 4.3 (Turkes and Tatli 2008, 2009). Drought is described without dividing it into being meteorological, agricultural and hydrological drought as “lack of water and/or water deficiency occurred when the level of

Table 4.3 Classification of the *SPI* values for calculating the climatological *SPI* probabilities

SPI values	Classification
≥ 2.00	Extremely wet
≥ 1.00	Above normal
> 0.0	Wet
$-0.99 - 0.99$	Normal
< 0.0	Dry
≤ -1.00	Below normal
≤ -2.00	Extremely dry

natural water availability used by several systems on the Earth surface is below long-term average or the normal level at the regional scale and for a particular time period. In general, drought events are considered as three dimensional natural events that are characterized with components of magnitude/severity, length/frequency and geographical distribution pattern" (Turkes 2010, 2013, 2017c).

Drought occurs in conjunction with climate change and variability in various time periods and may last consequently a few years or more than a few years. Drought has no one mean. Drought events are divided into four main groups; meteorological, agricultural, hydrological and socio-economical droughts. Description of a drought in general is the meteorological drought above mentioned. Agricultural drought occurs in conjunction with loss of soil moisture around plant root level, and it causes loss of plant and agricultural yield. Hydrological drought occurs in conjunction with the decreased amount or level of water, which is lower than amount demanded, in hydrological systems or in reservoirs in a region or district. Meteorological, agricultural and hydrological drought may turn into a socio-economical drought, when the magnitude of a drought event and the length of time period with drought increase. This state of a drought event is also related with low degree of coping ability of the system (agriculture, energy, ecosystem, urban and socio-economical, etc.), and lacks of drought risk management and drought management plans or weak implementation of these management plans (Turkes 2014b, 2017c).

Drought event is a serious threat effecting human life and health, socio-economic and ecological systems directly or indirectly at several degrees. Long-term drought events negatively affect agriculture, forestry, livestock, ecosystems, and hydroelectric energy, etc., by decreasing timely, qualified and sufficient water supplies. As a summary, the well-known adverse effects of geographically larger and significant drought events longer than 2 years can be listed as follows:

(i) Decreasing amount of ground water;
(ii) Decreasing water amount and level at stream-flows, reservoirs and water structures, etc.;
(iii) Increasing water pollution; salinization of water and soil;
(iv) Increasing soil pollution due to agricultural chemicals;
(v) Increasing soil erosion, land degradation and desertification;
(vi) Increasing the risk of wild bush and forest fires;

(vii) Damages to forest and rural wetland ecosystems and weakening and loss of biodiversity;

(viii) Increasing vulnerability level of natural vegetation and agricultural ecosystems due to adverse effects of disease, fires, wind deflation, and other related factors.

Spatial distributions of climatological probabilities for *below-normal* (the *SPI* values ≤ -1) monthly *SPI* values are illustrated in Fig. 4.14a. Maximum probabilities obtained for the below-normal conditions are nearly 0.35 on the Mediterranean cost of Turkey, and 0.37 along the Turkey-Syria border. On the other hand, throughout the Black Sea coastal region, the probabilities of being below-normal are generally 0.15 and a little below.

The probability of *being normal* (the *SPI* values within the interval of ± 1) reveals a spatial pattern where the displayed probabilities increase from the western and southern regions of Turkey (Fig. 4.14b), in which the Mediterranean rainfall regime with a high inter-seasonal and inter-annual variability is dominant, to the Black-Sea rainfall region, where the annual precipitation totals are greater and seasonality and year-to-year variability are lower than almost all of other regions of Turkey (Turkes

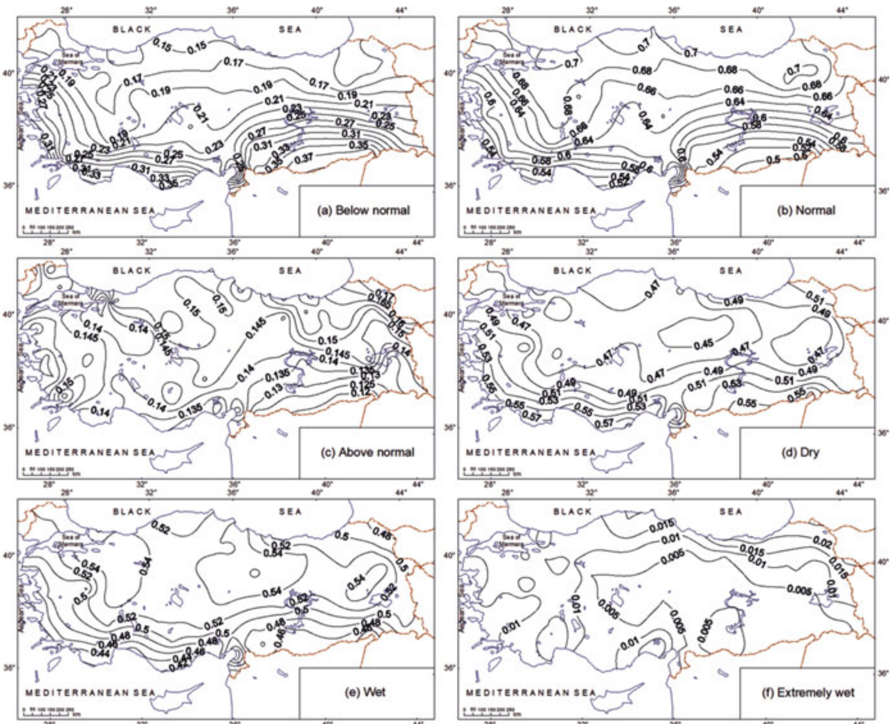

Fig. 4.14 Geographical distributions of the probabilities obtained for various *SPI* classes of monthly total precipitation series from 96 stations in Turkey. [Re-arranged in English from Turkes and Tatli (2008)]

1999, 2003, 2013). Probabilities of being normal over the central and the northern regions of the country have ratios varying from 0.65 to 0.70. Minimum probabilities of being normal are 0.52 on the Mediterranean coasts, and they are approximately 0.50 along the Turkey-Syria border.

The probabilities of being *above-normal* (the *SPI* values ≥ 1) show minima over the western and southern regions of Turkey (Fig. 4.14c), where the seasonality and inter-annual variability in total precipitation series are high in all seasons. The probabilities over these areas are within the interval of 0.12–0.14, and they decrease from the southern regions towards the coastal belt of the Black Sea rainfall region and the north-eastern Anatolia. These patterns are consistent with the previous studies of Turkes (1996, 1998, 2003, 2013, etc.) in terms of the main characteristics of the precipitation climatology in Turkey.

When the probabilities of monthly *SPI* values *being dry* (the *SPI* values <0) in general are considered, the probabilities of being dry are detected as 0.57 on the Mediterranean coastal belt and 0.55 over the Turkey-Syria border area. Probabilities tend to decrease from the Mediterranean rainfall region towards the north and reach a minimum value of 0.45 in the continental Central Anatolia Region (Fig. 4.14d).

The minimum probabilities of monthly *SPI* values *being wet* (the *SPI* values >0) in general are found as 0.44 over the Mediterranean coasts and 0.46 over the continental Mediterranean (South-eastern Anatolia) Region, whilst the probabilities of being wet reach a maximum level of about 0.54 over the eastern Marmara, western Black Sea, continental Central, and Eastern Anatolia rainfall regions (Fig. 4.14e).

The probabilities of *being extremely-wet* (the *SPI* values ≥ 2) are significantly low over Turkey, as is expected for most of the Mediterranean macro climate regions and more generally in the subtropical climate belt (Fig. 4.14f). The probabilities of being extremely-wet are at the level of 0.01 and below over the majority of Turkey. The maximum probabilities of being extremely-wet are about 0.02 in the middle and eastern Black Sea sub-regions and in the northern part of the north-eastern Anatolia sub-region, respectively.

One of the most significant and remarkable results for the *SPI* probabilities in Turkey is detected in the probabilities of *being extremely-dry* (the *SPI* values ≤ -2) (Fig. 4.15). The probabilities of being extremely-dry evidently depict maximum values on the Turkish shores of the Mediterranean Sea and over the border zone between Turkey and Syria with the highest probability of about 0.27 in the Harran and Akcakale plains, which are climatologically one of the most arid and desert-like environments of Turkey (Turkes 2003, 2013).

The probabilities of being extremely-dry reach their maximum values of about 0.21–0.23 on the Mediterranean coast of Turkey and 0.27 over the Turkey-Syria border. The estimated probabilities tend to decrease clearly from the southern regions towards the Black Sea shores. The lowest probabilities of being extremely-dry are detected as about 0.03 in the western and eastern Black Sea sub-regions and the north-eastern Anatolia sub-region of Turkey, respectively (Fig. 4.15).

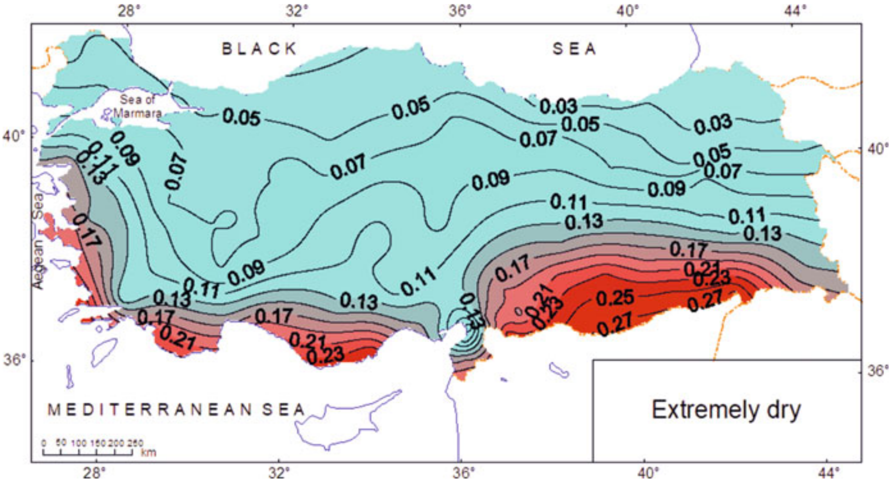

Fig. 4.15 Geographical distributions of the drought probabilities from the *Extremely-dry SPI* class of monthly total precipitation series from 96 stations in Turkey. [Re-arranged in English from Turkes and Tatli (2008)]

4.3.4 Drought Vulnerability and Risk

This sub-section aims at performing a vulnerability and risk assessment of Turkey based on a recent paper of Turkes (2017c), by considering the recent trends and approaches on the subject for disaster risk management of the weather and climate extremes and disasters towards climate change adaptation and reduction of its impacts.

Economic and social losses caused by weather and climate-related extreme events and disasters have been increasing with a great spatial and inter-annual variability in many regions of the world and in Turkey (Turkes and Erlat 2018b). The character, severity and impact powers of the extreme weather and climate events and disasters closely depend, not only on exposure and vulnerability levels that are varying across temporal and spatial scales, but also on economic, social, geographic, demographic, cultural, institutional, governance, and environmental and ecological factors (Turkes 2017c). A large part of Turkey is located over the dry-summer subtropical macro climate belt characterized with many climate and climate-related problems arising from its nature. In this respect, Turkey is a mid to high climate risk-prone country, with respect to not only the present climate and climate variability, but also to future climate change and variability. Turkey is also one of the South-eastern Europe and Eastern Mediterranean countries that are considerably vulnerable to desertification processes varying mid to high degrees (CEM 2017; Turkes 2017b, c).

In a study performed by Turkes (2017b), a Social Vulnerability Index (*SVI*) was used for determining "Turkey's 'Potential' Drought Hazard/Disaster Risk." The *SVI* is a tool that was originally developed and applied in the United States to help emergency response planners, public health experts, and officials geographically identify and map the communities that will most likely need support before, during, and after a hazardous event.

The estimation for Turkey's Vulnerability Index in terms of the impacts of drought events was based on five vulnerability factor classes including the following:

(i) Education status with one indicator (indicators not given here);
(ii) Demography with four indicators;
(iii) Economic activity with six indicators mostly related to agricultural activities and production;
(iv) Public health and health protection status and public coping capacities with five indicators;
(v) Natural environmental characteristics with three indicators.

In this frame, based on a well-known drought risk formula and the climatological drought occurrence probabilities estimated from the *SPI* series of Turkey, "Turkey's Drought Hazard/Disaster 'Potential' Risk Modelling and Valuation" was performed and mapped on the main administrative city provinces by using the spatial analysis tools of a geographical information system (GIS) (Fig. 4.16b).

When the socioeconomic and environmental conditions of the drought vulnerability in Turkey is considered, relatively the lowest and the highest vulnerability scores can be ranked as follows in terms of geographical regions, sub-regions, and the city provinces of Turkey (Fig. 4.16a):

The city provinces with relatively the lowest drought vulnerability levels include Edirne and Kirklareli provinces in the Western Thrace (European part of the Marmara Region); Bilecik, Bolu, Karabuk, Zonguldak and Bartin provinces in the Western Black Sea sub-region along with the city provinces in the Eastern Black Sea sub-region (Giresun, Trabzon, Rize and Artvin); and the Erzincan, Bayburt, Tunceli and Elazig provinces, and Erzurum and Ardahan provinces in the mid-west and north-east portions of the Eastern Anatolia Region, respectively (Fig. 4.16a). The city provinces with relatively the highest drought vulnerability scores consist of Istanbul and the surrounding cities, and Bursa in the Marmara Region in general. Others include Afyonkarahisar, Izmir and the surrounding city provinces except the provinces Mugla, Usak and Kutahya; Antalya, Adana, Hatay and Kahramanmaras provinces in the Mediterranean Region characterized with a true dry and hot summer Mediterranean climate, with a Köppen-Geiger climate (***Csa***), along with almost all city provinces in the South-eastern Anatolia Region with a continental Mediterranean rainfall regime (Gaziantep, Adiyaman, Sanliurfa, Diyarbakir, Mardin and Batman). This vulnerability level is seen also in almost all eastern and south-eastern portions of the Eastern Anatolia Region, including the cities of Sirnak, Mus, Van, Agri and Hakkari provinces (Fig. 4.16a).

Based on a special classification of the monthly *SPI* anomalies in order to estimate the drought risk of Turkey, Turkes (2017c) analyzed and evaluated the Drought Hazard-Disaster Risk (*DHDR*) under the conditions of Below-normal "Exact Drought Probability" for the administrative city provinces of Turkey (Fig. 4.16b). According to this special classification, relatively the lowest and the highest risk evaluations derived from the *DHDR* under the conditions of Below-normal "Exact Drought Probability" can be summarized as follows:

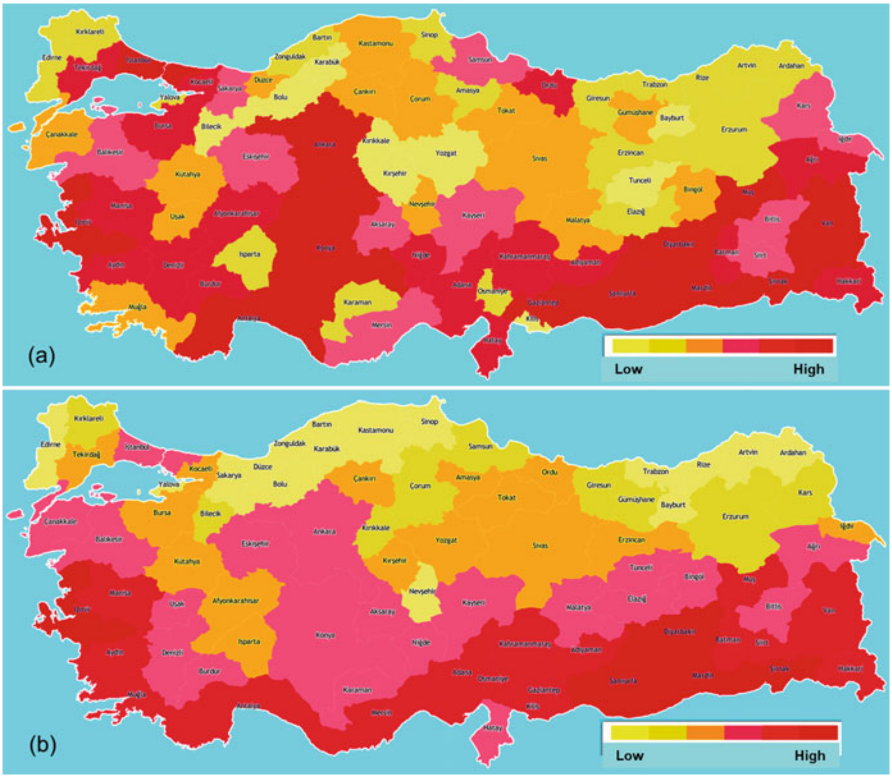

Fig. 4.16 Geographical distributions of (**a**) drought hazard-disaster *SVI* and of (**b**) evaluations for the Drought Hazard-Disaster Risk under the conditions of Below-normal "**Exact Drought Probability**" based on the *SPI*, both of which were estimated for Turkey's administrative city provinces. [Re-arranged in English from Turkes (2017b)]

The relatively highest *DHDR* scores of the geographical regions/sub-regions and the city provinces in Turkey are: Izmir (the highest), Manisa, Aydin and Mugla city provinces in the Aegean Region; Antalya, Mersin, Adana, Osmaniye and Kahramanmaras in the Mediterranean Region; Sanliurfa, Diyarbakir, Mardin (the highest ones) and Kilis, Gaziantep, Adiyaman, Siirt and Batman in the South-eastern Anatolia Region; Sirnak (the highest), Siirt, Hakkari, Van and Mus in the Eastern Anatolia Region; Ankara, Eskisehir, Konya, Aksaray, Karaman, Nigde and Kayseri in the Central Anatolia Region; and Istanbul, Canakkale and Balikesir in the Marmara Region, respectively (Fig. 4.16b). On the other hand, relatively the lowest *DHDR* levels of the geographical regions/sub-regions and the city provinces in Turkey under the conditions of Below-normal "Exact Drought Probability" consist of Edirne (the lowest) and Kirklareli in the Western Thrace of the Marmara Region along with Bilecik province of the Eastern Marmara sub-region; Corum, Samsun, Giresun and Gumushane and the all the city provinces from Sakarya to Rize and Artvin (the lowest ones) except the city provinces of Amasya, Tokat and Ordu in the

Black Sea Region; Nevsehir (the lowest), Kirikkale and Corum in the Central Anatolia Region; and Ardahan (the lowest), Kars and Erzurum in the Eastern Anatolia Region, respectively (Fig. 4.16b).

4.4 General Soil Characteristics of Turkey with Respect to Climate

4.4.1 Climate and Soil

Climate is usually considered the dominant factor on soil formation. However, the soil parent material still claims an impressive number of adherents. The natural topography and geomorphologic units, which are particular relief groups developed under the specific morphoclimatic or morphogenetic regions of the Earth, are also important for soil formation. In recent years, the role of vegetation in soil formation has aroused further interest. Yet, because systematic quantitative studies of the relationships between soil properties and all soil-forming factors have not been adequate yet to explain all these relationships, all the remaining factors can be kept constant in order to detect the role played by each soil-forming factor.

However, if we would consider the soil as a physical system as proposed by Jenny (1994), we may add substances to or remove from it, because the soil system is an open system. Every soil system is characterized by properties that we may designate by symbols, such as *s1, s2, s3, s4, s5*, etc. For example, *s1* may indicate nitrogen content, *s2* acidity, *s3* apparent density, *s4* amount of calcium (Ca), *s5* pressure of carbon dioxide (CO_2), etc. The simplest method of expressing the assumptions of interrelationships is given in form of the Eq. (4.2) as follows (Jenny 1994):

$$F\ (s1, s2, s3, s4, s5, \bullet\bullet\bullet) = 0 \tag{4.2}$$

On the other hand, when the soil and environment relationship is considered, it is generally realized that the soil system is only a part of a much larger system that is composed of the most upper part of the lithosphere, the lowest part of the atmosphere (i.e. lower troposphere), and a considerable part of the biosphere. Consequently, properties of the soil system that are universally recognized as soil characteristics should be considered. They include the following: soil climate (soil temperature and soil moisture, etc.), kind and number of soil organisms, and topography, or the shape of the surface of the soil system. These properties can be indicated by special symbols ($cl' =$ climate, $o' =$ organisms, $t' =$ topography) (Jenny 1994), which are included in the Eq. (4.3)) as:

$$F\left(cl', o', t', s1, s2, s3, \bullet\bullet\bullet\right) = 0 \tag{4.3}$$

The following set of individual equations of soil-forming factors can also be written:

$$s = fcl\ (climate)\ o, t, p, ti,\ \ldots \tag{4.4}$$

$$s = fo\ (organisms)\ cl, t, p, ti,\ \ldots \tag{4.5}$$

$$s = ft\ (topography)\ cl, o, p, ti,\ \ldots \tag{4.6}$$

$$s = fp\ (parent\ material)\ cl, o, t, ti,\ \ldots \tag{4.7}$$

$$s = fti\ (time)\ cl, o, t, p,\ \ldots \tag{4.8}$$

The subscripts indicate that the remaining soil-forming factors do not vary. For instance, in order to study accurately the soil-climate relationships, it is necessary that comparisons should be restricted to soils of identical origin and the time of soil formation, etc. On the other hand, the climate factor is so complex that no single numerical value can be assigned to a given climate. It becomes necessary to work with individual climatic variables, the most important of which are air humidity (H), air temperature (T), and soil moisture (m). Treating these three important climate elements as independent variables, an approximate equation may be written as follows:

$$s = f\ (H, T, m)\ o, t, p, ti,\ \ldots \tag{4.9}$$

4.4.2 Climate-Related Land Degradation

Soils in the semiarid and the dry-sub humid climate regions (drylands) of Turkey are vulnerable to land degradation, either because they have poor resistance to erosion, or because of their chemical and physical properties. A preliminary study on the soil moisture conditions of the soils in Turkey was published first by Caglar (1937). He investigated the soil-water relationships under the conditions of the continental Central Anatolia Region. The hydrology, climate, soil conditions, microorganisms and soil–water relations, the quality of water used for irrigation and characteristics of the waters in Turkey had also been discussed in this publication. In fact, the majority of the publications on soil water conservation studies in Turkey were concentrated on soil erosion in the past (e.g. Yamanlar 1956; Celebi 1970, 1971; Mermut et al. 1981, etc.). In this respect, for instance, sand dune rehabilitation studies were undertaken for the sand dune areas in Adana and Mersin-Tarsus districts of the Eastern Mediterranean sub-region of Turkey in order to enhance carbon sequestration and soil formation conditions at the stone pine canopies/root-zones of arenosols (Akca et al. 2010; Polat and Kapur 2010).

The most important and well-known soil degradation and desertification district in Turkey is Karapinar town (Konya). The Karapinar town is located over the plateaus and plains between in Konya and Eregli districts of Turkey. It is characterized with a semi-arid steppe climate of the continental Central Anatolia Region, and annual average precipitation amount is about 250–300 mm over the district (Turkes 1999, 2003, 2013). Because of the semi-arid climate, no forests naturally grew up in the district, and steppe vegetation dominated over the land. Consequently, the flat terrain had been used as a pasture for long years and especially sheep rising was practiced here. In areas where the vegetation was destroyed as a result of intensive grazing and drought events, the thin layer of the soil (mainly clay and silt) was removed (Groneman 1968). The remaining sand was removed by the wind deflation in short distances and turned the land into a large continental dune. So the ancient dune-like landscape was probably built up, mainly due to the fact that the native steppe vegetation was damaged by over grazing, trampling and by other human activities (Groneman 1968). The wind eroded parts of this ancient dune-like landscape altered it in many places and formed many blowouts. The shifting sand accumulated downwind and built up new dunes during the 1960s in many places (Fig. 4.17). In fact, this increasing activity in the continental dune field began to affect the Karapinar settlement as of 1956. Consequently, the Karapinar town and its some nearby villages had faced the danger of abandonment due to immigration in the early 1960s. Approximately 4300 hectare (ha) areas were covered with an inland dune in the south-southwest of the district, developed due to severe wind erosion and deflation (Groneman 1968; Carkaci 1999; Yildirim 1999; Akca et al. 2000; Yildirim and Akay 2010; Kantarci et al. 2011, etc.).

Fig. 4.17 The degraded land by strong wind erosion and deflation, and the Barkan-like Sand Dune formations in Karapinar district during the late 1950s and the 1960s. (Carkaci 1999)

Fig. 4.18 A general view of a nearby village of Karapinar Town in early 1960s. (Carkaci 1999)

Finally, the soils lost their yield capacity and sand dunes occurred as the result of erosion. It was observed that clouds of sand and dust storms rose, and vehicles on the Konya-Adana Highway were dragged, and the paint of the cars was totally or partially damaged. Children could not go to school because of sand storms, machines did not work, and the incidence of ear-nose-throat diseases increased among the people (Anonymous 2007). Winds that cause erosion in the district are mainly south-south-westerly. Finally, these significantly adverse conditions forced the local community to leave their places as they were threatened by this disaster (Fig. 4.18). Grazing and picking woody plants is still forbidden in the protected and reclamation areas. In the past, all the farmer villages had been vacated, except the village Kindam, which is situated about three kilometers southwest from Karapinar (Groneman 1968). Formerly, all the deserted villages had been summer camps (yayla in Turkish). In winter, the summer camps were deserted, and then the farmers started living in the towns.

Following this destruction, the necessary technical sand-dune preventing and/or controlling works and actions began in 1962/63 by the former General Directorate of Soil-Water, VI. Regional Directorate of Konya Soil-Water, Chief Engineering of Wind Erosion Plan and Application Group (Anonymous 2007, 2010; Carkaci 1999).

Reasons for the increased wind erosion and deflation in the Karapinar district can be summarized as follows (Groneman 1968; Carkaci 1999; Akca et al. 2000; Yildirim and Akay 2010; Kantarci et al. 2011):

- The sandy material originated from old lake bed mobilized, following the drying up of the lake;

- The hot and semi-arid continental climate conditions along with the high precipitation seasonality and year-to-year variability;
- Impetuous destruction of pastures because of overgrazing and the use of pasture plants for fuel,
- Excessive tillage, particularly by the Shock-Disc Plough that degrades the soil structure and buries productive surface horizon of the soil, and
- Karapinar is located on a strong wind course.

The first step taken against erosion in the district was the establishment of the "Association for Saving Karapinar from Erosion" in 1959. Afterwards, studies were started by the former Directorate of Konya Soil-Water Research Institute in 1962. A team was formed of technical personnel, and an area of 16,000 ha was taken under control by enclosing it with a wire fence. Then, 3000 ha of this area was assigned to the Turkish Armed Forces to be used for military purposes. The remaining 13,000 ha area was divided into four sections, based on the problems observed. Soil improvement practices started in this area considering the degree of the problem. The former Directorate of Konya Soil-Water Research Institute maintained its studies continuously for 10 years, and when the improvement studies were completed, the area was assigned to Konya Institute of Soil and Water Research Directorate in 1973 to be used for protection control, research and production studies. Today, 4300 ha of this land is given back to farmers, and studies are continued in the 8700 ha under the control of the government (Fig. 4.19) (Yildirim 1999). The research station in Karapinar town is now entitled as "Research Institute of the Directorate of Konya Soil and Water Resources".

Fig. 4.19 A present view of the Karapinar wind erosion area that has been opened to sustainable and productive agricultural practices for many years. (Photograph: Murat Turkes 17.06.2013)

4.4.3 Soil Geography

Generalized soil map of Turkey (Cullu et al. 2018), which is based on the World Reference Base for Soil Resources (WRB), is given in Fig. 4.20. These soil data compilations were subsequently analyzed in a GIS environment, and the soils were classified in accordance with the WRB (IUSS Working Group WRB 2015) procedures by Cullu et al. (2018), which are primarily intended to facilitate the correlation of national and local systems with international soil classification schemes.

According to this classification, the most widely distributed soils of Turkey (i.e. mapped WRB soil groups) are the Cambisols/Cambisols-Leptosols (63.55%), Fluvisols (9.50%), Calcisols/Calcisols-Leptosols (9.39%), Vertisols (5.15%), Alisols-Acrisols-Podsols (3.25%), Kastanozems (2.85%), and Luvisols (2.05%). The group of Cambisols/Cambisols-Leptosols is detected almost in all the geographical regions of Turkey, with the exception of the coastal zone of the Black Sea Region, south-west Anatolia, the mid-south part of the Central Anatolia Region, and the southern part of the South-eastern Anatolia Region, the last two regions of which are mainly characterized with the Calcisols/Calcisols-Leptosols soil groups. Cullu et al. (2018) pointed out that the Cambisols, Calcisols, Vertisols, and Fluvisols are the most appropriate and extensively managed soil ecosystems, particularly for field crops and cereals. Furthermore, the Calcisols, Luvisols, Acrisols-Alisols-Podsols, and Arenosols are significantly suitable for the production of some crops, such as the

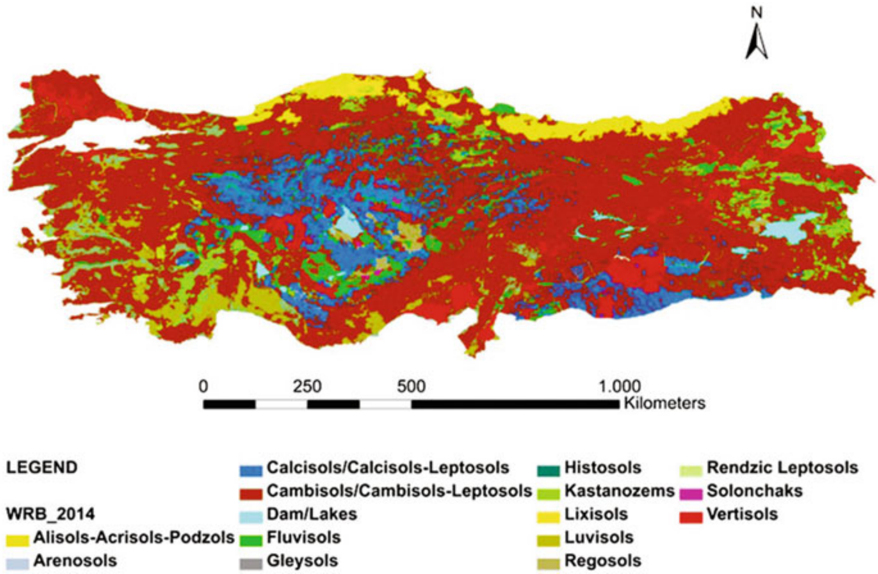

Fig. 4.20 Geographical distributions of the generalized WRB soil groups of Turkey. (Cullu et al. 2018)

olives, carobs, apricots, hazelnuts, and stone pine. On the other hand, because the Solonetz, Solonchaks, Gleysols, and Regosols are the most problematic soil ecosystems for agricultural production, they need to be treated by supplementary activities for sustainable use.

Acknowledgements The authors are grateful the NOAA/OAR/ESRL/PSD (Boulder, Colorado) for providing "the 20th Century Reanalysis V2 data" at "http://www.esrl.noaa.gov/psd/data/20thC_Rean/ and http://www.esrl.noaa.gov/psd/data/gridded/data.20thC_ReanV2.html", and the Turkish Meteorological Service for providing the climatological and meteorological data.

References

Akca E, Kapur S, Serin M, Cevik B, Eswaran H (2000) Karapinar: a case study of rehabilitation of a wind eroded area in Turkey. 13–17 June, 2000, Desertification meeting, Konya, pp 202–210

Akca E, Kapur S, Tanaka Y, Kaya Z, Bedestenci HC, Yakti S (2010) Afforestation effect on soil quality of sand dunes. Polish J Environ Stud 19(6):1109–1116

Anonymous (2007) Yeseren Col Karapinar. Republic of Turkey, Ministry of Agriculture and Rural Affairs, General Directorate of Agricultural Research, Soil and Water Resources Research Institute of Konya (in Turkish)

Anonymous (2010) Karapinar is greener now. Booklet. Konya Directorate of Research Station of Soil, Water and Combating Desertification, Karapinar, Konya

Barry RG, Chorley RJ (2003) Atmosphere, weather and climate, 8th edn. Routledge Taylor and Francis Group, London, 421 p

Çaglar KO (1937) Anadolu Sartlarina gore Su ve Toprak Munasebetlerinin Arastirilmasi. Ankara Yuksek Ziraat Enstitusu, Ankara

Carkaci A (1999) Examples of good practices of Turkey for combating wind erosion (Examples of Karapinar). Directorate of Research Institute of Soil Water and Combating Desertification, Karapinar, Konya

Celebi H (1970) The soil losses induced by wind erosion and some physical and chemical properties of soils of Sivas Ulas State Farm. Guven Publisher, Ankara. 46 p (in Turkish)

Celebi H (1971) Study on the resistance to soil erosion in the Kars meadow and Sarikamis Forest soils. Agric Eng 53:18–22 (in Turkish)

CEM (2017) Turkiye Collesme Modeli, Teknik Ozet. Collesme ve Erozyonla Mucadele (CEM) Genel Mudurlugu, Ankara

Coughlin KT, Tung KK (2001) QBO signal found at the extratropical surface through northern annular modes. Geophys Res Lett 28:4563–4566

Coughlin KT, Tung KK (2004) Eleven-year solar cycle signal throughout the lower atmosphere. J Geophys Res Atmos 109:D21105.1–D21105.7

Cullu MA, Gunal H, Akca E, Kapur S (2018) Soil geography. In: Kapur S, Akca E, Gunal H (eds) The soils of Turkey. Springer World Soils Book Series. Springer, pp 105–110. ISBN: 978-3-319-64390-8. https://doi.org/10.1007/978-3-319-64392-2

Dengiz O (2018) Potential impact of land use change on land productivity dynamics with focus on land degradation in a sub-humid terrestrial ecosystem. Theor Appl Climatol 133(1–2):73–88. https://doi.org/10.1007/s00704-017-2162-1

Elibuyuk M, Erkan Y (2010) Altitude steps and slope groups of Turkey in comparison with geographical regions and sub-regions. Cografi Bilimler Dergisi (J Geogr Sci) 8:27–55

Erinc S (1969) Klimatoloji ve Metodlari. Istanbul Universitesi Cografya Enstitusu, Yayin No. 35, Istanbul

Erinc S (1982) Jeomorfoloji, Cilt: I. Genisletilmis ucuncu baski. Istanbul Universitesi Edeb. Fak. Yay. No: 2931. Edebiyat Fakultesi Matbaasi, Istanbul
Erlat E, Turkes M (2012) Analysis of observed variability and trends in numbers of frost days in Turkey for the period 1950–2010. Int J Climatol 32(12):1889–1898. https://doi.org/10.1002/joc.2403
Erlat E, Turkes M (2013) Observed changes and trends in numbers of summer and tropical days, and the 2010 hot summer in Turkey. Int J Climatol 33(8):1898–1908. https://doi.org/10.1002/joc.3556
Erlat E, Turkes M (2016) Dates of frost onset, frost end and the frost-free season in Turkey: trends, variability and links to the North Atlantic and Arctic oscillation indices, 1950−2013. Clim Res 69:155–176. https://doi.org/10.3354/cr01397
Essenwanger OM (2001) Classification of climates. World survey of climatology volume 1C (General climatology 1C), Epilogue by Landsberg, H.E. Elsevier, Amsterdam
Groneman AF (1968) The soils of the wind erosion control camp area Karapinar, Turkey. A part of Great Konya Basin soil research and trainings project report, Vageningen
Guttman NB (1998) Comparing the palmer drought index and the standardized precipitationindex. J Am Water Resour Assoc 34:113–121
Guttman NB (1999) Accepting the standardized precipitation index: a calculation algorithm. J Am Water Resour Assoc 35:311–322
Henderson-Sellers A, Robinson PJ (1986) Contemporary climatology, 1st edn. Longman Scientific & Technical, Essex/New York, 439p
Huang NE, Shen Z, Long SR, Wu MC, Shih HH, Zheng Q, Yen NC, Tung CC, Liu HH (1998) The empirical mode decomposition and the Hilbert spectrum for nonlinear and nonstationary time series analysis. Proc R Soc London Ser A Math Phys Eng Sci 454:903–995
Ilhan E (1976) Geology of Turkey, ODTU Muhendislik Fakultesi Yayin No. 51, Ankara, 239 pp (in Turkish)
IUSS Working Group WRB (2015) World reference base for soil resources 2014, update 2015 international soil classification system for naming soils and creating legends for soil maps. World soil resources reports No. 106. FAO, Rome, 203p
Iyigun C, Turkes M, Batmaz I, Yozgatligil C, Gazi VP, Koc EK, Ozturk MZ (2013) Clustering current climate regions of Turkey by using a multivariate statistical method. Theor Appl Climatol 114:95–106. https://doi.org/10.1007/s00704-012-0823-7
Jenny H (1994) Factors of soil formation: a system of quantitative pedology. Foreword by Ronald Amundson. Dover Publications, New York
Kantarci MD, Ozel HB, Ertek M, Kirdar E (2011) An assessment on the adaptation of 6 tree species to steppe habitat during Konya-Karapinar sand-dune afforestations. Bartin Orman Fakultesi Dergisi (J Bartin For Fac) 13(19):107–127
Ketin I (1966) Anadolu'nun Tektonik Birlikleri. MTA Dergisi 66:20–34
Ketin I (1983) Turkiye Jeolojisine Genel Bir Bakis. Istanbul Teknik Universitesi (ITU) Kutuphanesi Sayi: 1259. ITU Matbaasi, Gumussuyu, Istanbul
Ketin I (1994) Genel Jeoloji, Yerbilimlerine Giris. Dorduncu Baski, Istanbul Teknik Universitesi (ITU) Vakfi Yayinlari No. 22, Istanbul
Köppen W (1936) Das geographisca System der Klimate. In: Kööppen W, Geiger G (eds) Handbuch der Klimatologie. 1. C. Gebr, Borntraeger, pp 1–44
Köppen W, Geiger G (1954) Klima der Erde (map). Justus Perthes, Darmstadt, Germany. American distributor, A. J. Nystrom, Chicago
Kutiel H, Turkes M (2005) New evidence about the role of the North Sea – Caspian pattern (*NCP*) on the temperature and precipitation regimes in continental Central Turkey. Geogr Ann Ser B 87:501–513
Kutiel H, Hirsch-Eshkol TR, Turkes M (2001) Sea level pressure patterns associated with dry or wet monthly rainfall conditions in Turkey. Theor Appl Climatol 69:39–67
Lolis CJ, Turkes M (2016) Atmospheric circulation characteristics favoring extreme precipitation in Turkey. Clim Res 71:139–153. https://doi.org/10.3354/cr01433

McKee TB, Doesken NJ, Kleist J (1993) The relationship of drought frequency and duration of time scales. Presented at the eighth conference on applied climatology. American Meteorological Society, Anaheim CA, pp 179–186
McKee TB, Doesken NJ, Kleist J (1995) Drought monitoring with multiple time scales. Presented at the ninth conference on applied climatology. American Meteorological Society, Dallas TX, pp 233–236
Mermut AR, Tanju O, Hatipoglu F, Baskaya HS, Aktas M (1981) Annotated bibliography on Turkish soil science 1928–1976. Documentation of Turkish Research and Technical Centre, 1007 p (in Turkish)
Ozturk T, Altinsoy H, Turkes M, Kurnaz ML (2012) Simulation of temperature and precipitation climatology for Central Asia CORDEX domain by using RegCM 4.0. Clim Res 52:63–76. https://doi.org/10.3354/cr01082
Ozturk T, Ceber ZP, Turkes M, Kurnaz ML (2015) Projections of climate change in the Mediterranean Basin by using downscaled global climate model outputs. Int J Climatol 35:4276–4292. https://doi.org/10.1002/joc.4285
Peel MC, Finlayson BL, McMahon T (2007) Updated world map of the Köppen-Geiger climate classification. Hydro Earth Syst Sci 11:1633–1644
Polat O, Kapur S (2010) Soil quality parameters in Arenosols under Stone Pine (Pinus pinea L.) plantations in the Turan Emeksiz sand dune Area. Cukurova University, Institute of Science. J Sci Eng 3(2):167–174. Adana (in Turkish)
Russell RJ (1931) Dry climates of the United States: I climatic map. Univ Calif Publ Geogr 5:1–41
Sahin S, Turkes M, Wang S-H, Hannah D, Eastwood W (2015) Large scale moisture flux characteristics of the Mediterranean basin and their relationships with drier and wetter climate conditions. Clim Dyn 45(11):3381–3401. https://doi.org/10.1007/s00382-015-2545-x
Sen B, Topcu S, Turkes M, Sen B, Warner JF (2012) Projecting climate change, drought conditions and crop productivity in Turkey. Clim Res 52:175–191. https://doi.org/10.3354/cr01074
Sengor AMC (1980) Turkiye'nin Neotektoniginin Esaslari. Turkiye Jeoloji Kurumu Yayini. DSI Basim ve Foto-Film Isletme Mudurlugu Matbaasi, Ankara
Strahler AN (1973) Introduction to physical geography, 3rd edn. Wiley, New York
Thom HCS (1966) Some methods of climatological analysis. Technical note no. 81. WMO, Geneva
Thornthwaite CW (1948) An approach toward a rational classification of climate. Geogr Rev 38:55–94
Topcu S, Sen B, Turkes M, Sen B (2010) Observed and projected changes in drought conditions of Turkey. In: Options Méditerranéennes, Series A, Mediterranean Seminars 2010, No. 95 – Economies of drought and drought preparedness in a climate change context. CIHEAM, Paris, pp 123–127
Trigo R, Xoplaki E, Zorita E, Luterbacher J, Krichak S, Alpert P, Jacobeit J, Saenz J, Fernandez J, Gonzalez-Rouco F, Garcia-Herrera R, Rodo X, Brunetti M, Nanni T, Maugeri M, Turkes M, Gimeno L, Ribera P, Brunet M, Trigo I, Crepon M, Mariotti A (2006) Chapter 3: Relations between variability in the Mediterranean region and mid-latitude variability. In: Lionello P, Malanotte-Rizzoli P, Boscolo R (eds) Mediterranean climate variability. Elsevier Developments in Earth & Environmental Sciences 4, Amsterdam, pp 179–226
Turkes M (1996) Spatial and temporal analysis of annual rainfall variations in Turkey. Int J Climatol 16:1057–1076
Turkes M (1998) Influence of geopotential heights, cyclone frequency and southern oscillation on rainfall variations in Turkey. Int J Climatol 18:649–680
Turkes M (1999) Vulnerability of Turkey to desertification with respect to precipitation and aridity conditions. Turk J Eng Environ Sci 23:363–380
Turkes M (2003) Spatial and temporal variations in precipitation and aridity index series of Turkey. In: Bolle HJ (ed) Mediterranean climate – variability and trends, Regional climate studies. Springer, Heidelberg, pp 181–213
Turkes M (2010) Climatology and meteorology, 1st edn. Kriter Publisher – Publication No. 63, Physical Geography Series No. 1. ISBN: 978-605-5863-39-6, 650 + XXII pp., Istanbul (in Turkish)

Turkes M (2013) Iklim Verileri Kullanilarak Turkiye'nin Collesme Haritasi Dokumani Hazirlanmasi Raporu. Birinci Baski, T.C. Orman ve Su Isleri Bakanligi, Collesme ve Erozyonla Mucadele Genel Mudurlugu Yayini, ISBN: 978-6054610-51-8, 57p, Ankara

Turkes M (2014a) Kuraklik Olaylarinin Iklim Degisikligi ve Collesme Acisindan Onemi ve Turkiye'deki 2013–2014(?) Kurakliginin Sinoptik Klimatolojik/Meteorolojik ve Atmosferik Baglantilari. 3 Mart 2014. Hidropolitik Akademi Iklim Degisikligi ve Kuraklik Calismalari, Ankara. http://www.hidropolitikakademi.org/wp-content/uploads/2014/03/Climate_Change_2014_and_Dara_C%C3%B6llesme.pdf

Turkes M (2014b) Turkiye'deki 2013-2014 kurakliginin ve klimatolojik/meteorolojik nedenlerinin cozumlenmesi (Analysis of 2013-2014 drought in Turkey and its climatological and meteorological reasons). Konya Toprak Su Dergisi 2:20–34 (in Turkish and English)

Turkes M (2016) Kuresel Iklim Degisiklikleri ve Baslica Nedenleri ile Dunya'da ve Turkiye'de Gozlenen ve Ongorulen Iklim Degisiklikleri ve Degiskenligi. Icinde: "Kuresel Iklim Degisikligi ve Etkileri" Engin Ural Anisina (Ed: M. Somuncu). Turkiye Cevre Vakfi Yayini, Ankara, pp 71–115

Turkes M (2017a). General climatology: fundamentals of atmosphere, weather and climate, revised 2nd edn. Kriter Publisher Physical Geography Series No. 4. ISBN: 978-605-9336-28-4, xxiv + 520 p, Kriter Publisher, Berdan Matbaasi, Istanbul (in Turkish)

Turkes M (2017b) Birlesmis Milletler Collesme ile Savasim Sozlesmesi ve Turkiye'nin Durumu-Uyumu. Icinde: Uluslararasi Cevre Rejimleri (Der. G. Orhan, S. C. Mazlum, Y. Kaya), 1. Baski, pp 169–197. Dora Basim-Yayin Dagitim Ltd. Sti., Bursa. ISBN: 9789752447530

Turkes M (2017c) Drought vulnerability and risk analysis of Turkey with respect to climatic variability and socio-ecological indicators. Ege Cografya Dergisi 26(2):47–70 (in Turkish with an English abstract, figure and table captions)

Turkes M, Akgunduz AS (2011) Assessment of the desertification vulnerability of the Cappadocian district (Central Anatolia, Turkey) based on aridity and climate-process system. Int J Hum Sci 8:1234–1268

Turkes M, Erlat E (2003) Precipitation changes and variability in Turkey linked to the North Atlantic oscillation during the period 1930-2000. Int J Climatol 23:1771–1796

Turkes M, Erlat E (2005) Climatological responses of winter precipitation in Turkey to variability of the North Atlantic oscillation during the period 1930-2001. Theor Appl Climatol 81:45–69

Turkes M, Erlat E (2006) Influences of the North Atlantic oscillation on precipitation variability and changes in Turkey. Nuovo Cimento Della Societa Italiana Di Fisica C-Geophysics and Space Physics 29:117–135. https://doi.org/10.1393/ncc/i2005-10228-8

Turkes M, Erlat E (2008) Influence of the Arctic oscillation on variability of winter mean temperatures in Turkey. Theor Appl Climatol 92:75–85. https://doi.org/10.1007/s00704-007-0310-8

Turkes M, Erlat E (2009) Winter mean temperature variability in Turkey associated with the North Atlantic oscillation. Meteorog Atmos Phys 105:211–225. https://doi.org/10.1007/s00703-009-0046-3

Turkes M, Erlat E (2018a) Observed change and trends in record and absolute maximum and minimum air temperatures of Turkey during 1950-2015, and associated atmospheric conditions favouring these variations. Int J Climatol Accepted, in print

Turkes M, Erlat E (2018b) A scientific assessment of observed changes and trends in extreme weather and climate events in the world and Turkey. In: Ucal M (ed) Climate change and green perspective: green economy, green growth. Heinrich Böll Stiftung Foundation, Istanbul, pp 5–38

Turkes M, Tatli H (2008) Turkiye'de kuraklik olasiliklarinin standartlastirilmis yagis indisi (SPI) kullanilarak saptanmasi ve iklimsel degiskenlik acisindan degerlendirilmesi. Kuresel Iklim Degisimi ve Su Sorunlarinin Cozumunde Ormanlar Sempozyumu Bildiriler Kitabi (Ed., Ünal Akkemik), 13–14 Aralik 2007. Istanbul Universitesi Orman Fakultesi, Istanbul, pp 55–62

Turkes M, Tatli H (2009) Use of the standardized precipitation index (SPI) and modified SPI for shaping the drought probabilities over Turkey. Int J Climatol 29:2270–2282

Turkes M, Sumer UM, Kilic G (2002a) Persistence and periodicity in the precipitation series of Turkey and associations with 500 hPa geopotential heights. Clim Res 21:59–81
Turkes M, Sumer UM, Demir I (2002b) Re-evaluation of trends and changes in mean, maximum and minimum temperatures of Turkey for the period 1929-1999. Int J Climatol 22:947–977
Turkes M, Koc T, Saris F (2009) Spatiotemporal variability of precipitation total series over Turkey. Int J Climatol 29:1056–1074
Turkes M, Kurnaz ML, Ozturk T, Altinsoy H (2011) Climate changes versus 'security and peace' in the Mediterranean macroclimate region: are they correlated? In: Proceedings of International human security conference on human security: new challenges, new perspectives, 27–28 October 2011, Istanbul, pp 625–639
TurkStat (2016) Turkey in statistics, 2015. Turkish Statistical Institute, Publication Number 4431, Printing Division, Ankara
Turuncoglu UU, Turkes M, Bozkurt D, Onol B, Sen OL, Dalfes HN (2018) Climate of Turkey. In: Kapur S, Akca E, Gunal H (eds) The soils of Turkey. Springer World Soils Book Series. Springer, pp 25–44. ISBN: 978–3–319-64390-8. https://doi.org/10.1007/978-3-319-64392-2
UNCCD (1995) The United Nations convention to combat desertification in those countries experiencing serious drought and/or desertification, particularly in Africa. Text with annexes. United Nations Environment Programme (UNEP), Geneva
UNEP (1993) World atlas of desertification. United Nations Environment Programme (UNEP), London
Wilcock AA (1968) Köppen after fifty years. Ann Assoc Am Geogr 58:12–28
Wilks DS (1995) Statistical methods in the atmospheric sciences: an introduction. Academic Press, San Diego
Willmott CJ (1977) WATBUG: a FORTRAN IV algorithm for calculating the climatic water budget. University of Delaware, Delaware
Wu ZH, Huang NE, Long SR, Peng CK (2007) On the trend, detrending, and variability of nonlinear and nonstationary time series. Proc Natl Acad Sci USA 104:14889–14894
Xoplaki E (2002) Climate variability over the Mediterranean. PhD dissertation. University of Bern, Switzerland
Xoplaki E, Gonz'alez-Rouco JF, Luterbacher J, Wanner H (2004) Wet season Mediterranean precipitation variability: influence of large scale dynamics. Clim Dyn 23:63–78
Yamanlar O (1956) Land classification on the basis of soil conservation in Marmara Region, Turkey with special reference to Yalova district. Istanbul Univ Pub. No. 697. Fac Forest No. 42, 98 p (in Turkish)
Yildirim AI (1999) The greening desert Karapinar. In: Cereal symposium, June 8–11, 1999, Konya, pp 440–448 (in Turkish)
Yildirim AI, Akay A (2010) The greening desert of Karapinar: an example from Turkey. In: Second International symposium on sustainable development, International Burch University-IBU Campus, Sarajevo, pp 546–551
Zhu X, Shen Z, Eckermann SD, Bittner M, Hirota I, Yee JH (1997) Gravity wave characteristics in the middle atmosphere derived from the empirical mode decomposition method. Geophys Res Lett 102:16545–16561
Zhu X, Yee JH, Talaat ER (2001) Diagnosis of dynamics and energy balance in the mesosphere and lower thermosphere. J Atmos Sci 58:2441–2454

Internet References

http://www.esrl.noaa.gov/psd/data/20thC_Rean/
http://www.esrl.noaa.gov/psd/data/gridded/data.20thC_ReanV2.html